The Stairway to Infinity: A Holographic Renormalization Flow from Noncommutative Scanning to the Langlands Program

Haobo Ma (Auric)*
AELF PTE LTD.
#14-02, Marina Bay Financial Centre Tower 1, 8 Marina Blvd, Singapore 018981

December 23, 2025

Abstract

We propose a *holographic renormalization-flow* framework for an auditable passage from finite-resolution readout data to arithmetic rigidity and further to automorphic (Langlands) semantics. Unlike a purely static "constitution" of objects and axioms, the present work treats the *climb itself* as the core mathematical object: starting from a noncommutative scan algebra (a Weyl pair and the irrational rotation C^*-algebra / noncommutative torus), we pass through the modular geodesic flow on the modular surface and its Gauss-map suspension (continued fractions as canonical cross-scale digits), reach the cusp interface where analytic data freezes into integer coefficient spectra via the q-expansion, and close the discrete layer by the prime-generated Hecke algebra and its multiplicative/recursive constraints. We give a slice–coefficient reconstruction identity valid at any height $y > 0$, together with a finite-N scan-sampling estimator whose error is explicitly controlled by star discrepancy and Ostrowski digits. Incorporating finite-alphabet readout, we obtain a sampling+quantization recovery bound and an exact integer-recovery-by-rounding criterion for arithmetic spectra. Finally, we provide a precise symmetry template for scale exchange: the modular S-inversion identifies endpoints on the modular curve (deep/shallow cusp) and corresponds, on the noncommutative torus side, to Morita/Fourier-type equivalences that exchange scan and readout roles.

Keywords: noncommutative geometry, irrational rotation algebra, noncommutative torus, modular curve, modular surface, geodesic flow, Gauss map, continued fractions, Ostrowski/ Zeckendorf coding, q-expansion, Hecke operators, automorphic forms, Langlands program, Morita equivalence, induced measure, discrepancy, S-duality.

Conventions. Unless otherwise stated, log denotes the natural logarithm. "mod 1" refers to reduction in $\mathbb{R}/\mathbb{Z}$. "Tick time" $t \in \mathbb{Z}_{\geq 0}$ denotes the iteration count of a scan operator. We write $\tau = x + \mathrm{i}y \in \mathbb{H}$ with $y > 0$ and use the cusp coordinate $q = \mathrm{e}^{2\pi\mathrm{i}\tau}$. When convenient, we freely replace $[0, 1)$ by $[0, 1]$ in integrals and discrepancy definitions, since the boundary has Lebesgue measure zero.

Contents

*Email: auric@aelf.io

1 Introduction: from a constitution to a climb

Modern foundational physics lives in a persistent tension. At the microscopic level, the canonical language is unitary evolution: continuous, reversible, and information-preserving. At the observational level, however, what is actually recorded is finite-resolution, discrete, and statistical: bits, integer labels, and counting data. The standard narrative attributes continuity to "ontology" (states, fields) and discreteness/probability to an externally imposed measurement postulate.

This work takes the opposite organizational stance: *readout is part of the structure*. Time, probability, and discreteness are required to arise within an explicit scan–projection protocol, under finite-resolution constraints, in a way that is auditable down to a concrete dependency chain. In earlier HPA–Ω manuscripts [1,2], this stance was articulated as a stratified audit rule: Layer 0 (states and algebras only), Layer 1 (protocols: scanning, readout, induced statistics), and Layer 2 (semantic interpretation: spacetime narratives), with the prohibition that Layer 2 may not be used as a premise of Layer 0/1 derivations.

There remains, however, a missing component. A constitution of objects and axioms identifies a stage and its allowed moves, but does not describe the *climb*: how scale is raised, how noise is filtered, how continuous analytic data freezes into integer spectra at the cusp interface, and how distinct scale descriptions can be short-circuited by symmetries and equivalences. The goal of this paper is to make the vertical axis into a computable object, by organizing a closed chain:

$$\begin{aligned} &\text{noncommutative scan (Weyl pair / } A_\alpha) \\ &\Longrightarrow \text{ modular renormalization flow (geodesic flow / Gauss map)} \\ &\Longrightarrow \text{ cusp interface } (q\text{-expansion}) \\ &\Longrightarrow \text{ Hecke dynamics (prime skeleton)} \\ &\Longrightarrow \text{ automorphic spectrum (Langlands semantics).} \end{aligned} \tag{1}$$

The key novelty is that the *cross-scale step* in (1) is not left as metaphor. We select the modular surface as a canonical mother space and use its geodesic flow—equivalently, the Gauss-map suspension flow on $(0,1)$—as a renormalization flow whose discrete return digits are continued-fraction coefficients. This makes canonical interfaces (continued fractions, Ostrowski coding, Zeckendorf on the golden branch) unavoidable rather than ad hoc.

What this paper adds. Building on the existing scan–projection and cusp/Hecke interface, we add four concrete ingredients.

- **A renormalization-flow object.** The modular geodesic flow provides an intrinsic cross-scale dynamic, with a computable "scale time" given by the roof function of the Gauss suspension.
- **A slice–coefficient reconstruction identity.** We show that q-expansion coefficients can be recovered from any height slice $y > 0$ by a Fourier projection (Section 5).
- **A finite-N coefficient estimator at finite resolution.** Replacing the slice integral by scan-orbit sampling yields a coefficient estimator whose error is controlled by star discrepancy and, via Ostrowski digits, by a local syntactic sum. Incorporating finite-alphabet readout, we obtain an explicit sampling+quantization bound and an exact recovery-by-rounding criterion for integer spectra (Section 9).
- **A scale-exchange symmetry template.** The modular S-inversion identifies cusp endpoints on $X(1)$ and exchanges deep/shallow regimes; on the noncommutative side, the corresponding $\mathrm{SL}_2(\mathbb{Z})$ action appears as Morita equivalence and Fourier exchange, abstractly realizing a scan–readout swap.

Layer discipline. We emphasize throughout that statements about "UV/IR", "wormholes", or "scale shortcuts" are *interpretation-layer* narratives. The derivations in this paper are conducted entirely in Layer 0/1 language: algebras, flows, digit laws, Fourier projections, and Hecke constraints.

2 Layering and axioms: the audit rule

To prevent interpretive narratives from being silently used as derivations, we keep the logic auditable by explicitly separating three layers.

Layer 0 (ontological layer). Only the language of *states and algebras* is allowed. No external time parameter and no external probability postulate is introduced.

Layer 1 (protocol layer). One may choose a scan and readout protocol under finite resolution. Operational time and statistics are defined *within* the protocol.

Layer 2 (interpretation layer). One maps Layer 1 structures to semantic narratives (spacetime, particles, gravity, entanglement). This layer is marked interpretive and may not be used as a premise in Layer 0/1 arguments.

This stratification is consistent with the broader HPA–Ω program [1, 2] and is adopted here as a strict audit rule.

Figure 1 summarizes the layer separation and highlights the one-way dependency: Layer 2 interpretation may annotate, but may not be used as a premise.

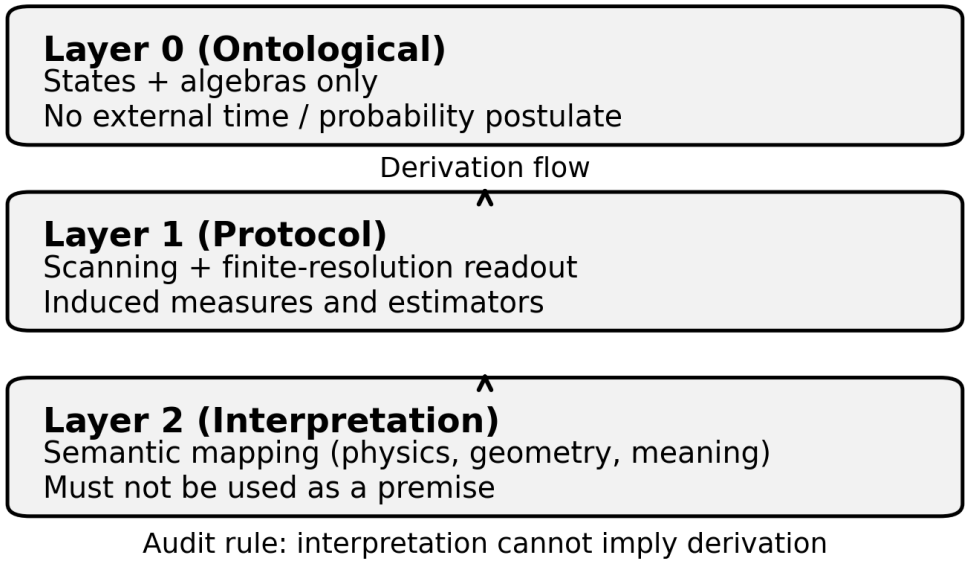

Figure 1: Layer separation and the audit rule. Layer 0 uses only states and algebras; Layer 1 specifies scanning, estimators, and finite-resolution readout; Layer 2 provides semantic interpretations and is explicitly excluded from the derivation chain.

2.1 Basic axioms (Omega O1–O4)

Axiom 2.1 (O1 (Omega: static global state))**.** *The universe is specified by a quasi-local operator algebra $\mathcal{A}$ together with a unique normalized global state ω_Ω on $\mathcal{A}$. There is no externally given*

time-indexed family of states.

Remark 2.2 (status and usage)**.** *Axiom O1 is a constitutive postulate of the broader HPA–Ω program. In algebraic settings, one may think of ω_Ω as a distinguished reference state (e.g. vacuum/KMS-type) selected by the model, rather than as an observer-defined ensemble; see, e.g., [3, 4]. The present manuscript's closed Layer 0/1 stairway chain does not use uniqueness of ω_Ω as an input: all quantitative recovery statements are derived at the protocol layer from O5/O6 and standard modular/ergodic theory (Appendix A).*

Axiom 2.3 (O2 (finite information))**.** *For any causally closed region, the effective number of degrees of freedom is bounded by a holographic constraint, typically of the form*

$$\dim \mathcal{H}_{\text{region}} \leq \exp\left(\frac{A}{4\ell_P^2}\right), \tag{2}$$

where A is an appropriate boundary area and ℓ_P is the Planck length.

Remark 2.4. *For standard reviews of holographic bounds and related formulations of the holographic principle, see, e.g., [5].*

Axiom 2.5 (O3 (causally local discrete update))**.** *There exists a discrete-step automorphism $\mathcal{U} : \mathcal{A} \to \mathcal{A}$ which, in a controlled representation, is implemented by a unitary U and has finite propagation range (a causal locality condition).*

Axiom 2.6 (O4 (holographic map))**.** *There exists a bulk-to-boundary encoding map Φ which is approximately isometric on an appropriate code subspace and supports reconstruction in the sense of algebraic quantum error correction / entanglement wedge reconstruction.*

Remark 2.7. *For standard constructions connecting holography, bulk reconstruction, and quantum error correction, see, e.g., [6–8].*

Remark 2.8 (scope in this paper)**.** *The core stairway results of this manuscript concern finite-resolution scan/readout protocols and the modular cusp/Hecke closure mechanism. Accordingly, O2–O4 serve primarily to situate the protocol layer within a holography-compatible constitution; they are not invoked in the proofs of the coefficient recovery bounds or Hecke closure checks.*

2.2 Upgraded axioms: scan–projection readout and Weyl pairs (O5–O6)

Axiom 2.9 (O5 (scan–projection readout and induced measures))**.** *Finite observers obtain "time" and "probability" from a finite-resolution scan and projection readout of intrinsic phase data. There exists a pointer phase $x \in \mathbb{R}/\mathbb{Z}$ whose scan orbit is sampled at integer ticks $t \in \mathbb{Z}_{\geq 0}$ by*

$$x_t = x_0 + t\alpha \pmod 1, \qquad \alpha \notin \mathbb{Q}. \tag{3}$$

Finite-resolution readout is described by a family of effects $\{E_k^{(\varepsilon)}\}$ (resolution parameter ε) inducing probabilities

$$P_k^{(\varepsilon)} = \omega_{\text{eff}}\left(E_k^{(\varepsilon)}\right), \qquad \sum_k E_k^{(\varepsilon)} = \mathbf{1}, \tag{4}$$

where ω_{eff} denotes the effective state in the observer sector.

Remark 2.10 (measurement-theory interface)**.** *The family $\{E_k^{(\varepsilon)}\}$ is a POVM in the standard sense, and $E \mapsto \omega_{\text{eff}}(E)$ is a state on the corresponding effect algebra; see [9, 10] for standard foundations. In algebraic formulations, one may regard ω_{eff} as a restriction of ω_Ω to an observer-accessible subalgebra (or via conditional expectations), recovering reduced-state pictures when tensor factorizations are available; see [3, 4].*

Axiom 2.11 (O6 (unitary scan algebra: a Weyl pair))**.** *On an effective observer Hilbert space $\mathcal{H}_{\mathrm{eff}}$, there exist a scan unitary U_{scan} and a conjugate phase unitary V satisfying the Weyl relation*

$$U_{\mathrm{scan}} V = \mathrm{e}^{2\pi \mathrm{i}\alpha} V U_{\mathrm{scan}}. \tag{5}$$

A canonical covariant model is given on $L^2(\mathbb{R}/\mathbb{Z})$ by

$$(U_{\mathrm{scan}}\psi)(x) = \psi(x+\alpha), \qquad (V\psi)(x) = \mathrm{e}^{2\pi \mathrm{i} x}\psi(x). \tag{6}$$

Assumption 2.12 (R1 (orbit regularization / finite part))**.** *Regulated-to-continuum passages along scan orbits are fixed by a canonical regularization convention: "Abel first, then limit", which selects a unique finite part for orbit traces and related divergent sums when it exists.*

Remark 2.13. *Abel summability and "Abel first, then limit" regularization are classical summability prescriptions; see [11].*

Remark 2.14 (scope of R1)**.** *The main finite-N recovery bounds in this paper are statements about finite sample averages and discrepancy control, and therefore do not require Assumption R1. R1 becomes relevant when one studies regulated infinite-time orbit traces, distributional limits, or boundary limits in which a damping parameter is sent to 1^- before taking a continuum limit (Appendix D.8).*

2.3 From constitution to climb: fixing a renormalization-flow object

To turn a static interface into a *cross-scale climb*, we must choose a geometric mother space together with an intrinsic flow that produces a computable notion of "scale time". We make the following canonical choice.

Mother space. We work with the modular curve

$$X(1) = \mathrm{PSL}_2(\mathbb{Z})\backslash(\mathbb{H} \cup \{\text{cusps}\}) \tag{7}$$

and the modular surface

$$M = \mathrm{PSL}_2(\mathbb{Z})\backslash\mathbb{H}. \tag{8}$$

The cusp structure of $X(1)$ has a single cusp class; in particular, the modular inversion $S : \tau \mapsto -1/\tau$ exchanges 0 and ∞ and identifies them in the quotient.

Remark 2.15 (why $X(1)$ (minimal protocol footprint))**.** *The role of the mother space is to provide (i) a cusp with a canonical q-coordinate for a continuous–discrete interface, (ii) a canonical climb with digit syntax via the Gauss/geodesic suspension, and (iii) a prime-indexed correspondence algebra (Hecke) closing the discrete layer. Within congruence covers, the one-cusp requirement is already rigid: proper congruence subgroups have multiple cusps, so $X(1)$ is the unique level 1 one-cusp option (Proposition C.1). For non-arithmetic quotients, the commensurator is discrete and Hecke correspondences do not produce a prime skeleton, blocking the intended closure [12]. Further discussion and a worked protocol model are given in Appendix C.1 and Appendix C.2.*

Flow. The geodesic flow on T^1M admits a canonical symbolic coding by continued fractions, via a Poincaré section whose first-return map is measurably conjugate to the Gauss map on $(0,1)$ [13]. The roof function of the corresponding suspension provides a computable additive "scale time" (recorded in Section 4).

This choice pins down the climb in Layer 1 terms: the same slope parameter α that controls scan readout also determines a continued-fraction digit sequence under Gauss iteration, and these digits become the local syntax of cross-scale coding.

3 Bottom layer: noncommutative scanning and finite-resolution readout

3.1 The irrational rotation algebra as the minimal scan closure

Under the Weyl relation of Axiom O6, the smallest C^*-algebraic closure generated by the scan/readout unitaries is the *irrational rotation algebra* (the standard noncommutative 2-torus)

$$A_\alpha := C^*\langle U, V \mid UV = \mathrm{e}^{2\pi \mathrm{i}\alpha} VU\rangle, \qquad \alpha \in (0,1)\setminus\mathbb{Q}, \tag{9}$$

studied classically by Rieffel and Connes [14, 15]. In the protocol semantics, U is a tick shift (scan iteration) and V is a pointer phase unitary, while the noncommutativity in (9) encodes intrinsic incompatibility between "scan time" and "readout phase".

Remark 3.1 (rigidity of the irrational rotation algebra)**.** *For irrational α, the rotation algebra A_α is simple and admits a unique tracial state; it is a canonical, rigid noncommutative geometric object associated with an irrational slope [14, 15].*

Proposition 3.2 (no simultaneous eigenvector)**.** *Let $\alpha \notin \mathbb{Q}$ and let U, V be unitaries satisfying $UV = \mathrm{e}^{2\pi\mathrm{i}\alpha}VU$. Then there is no nonzero vector ψ such that $U\psi = \lambda\psi$ and $V\psi = \mu\psi$ for some $\lambda, \mu \in \mathbb{C}$.*

Proof. If such ψ existed, then $UV\psi = \lambda\mu\psi$ and $VU\psi = \mu\lambda\psi$. The Weyl relation yields $\lambda\mu = \mathrm{e}^{2\pi\mathrm{i}\alpha}\mu\lambda$. Since $|\lambda| = |\mu| = 1$ and $\mathrm{e}^{2\pi\mathrm{i}\alpha} \neq 1$ for $\alpha \notin \mathbb{Q}$, this is impossible. □

3.2 A canonical covariant model on the circle

A standard realization of (9) is on $\mathcal{H} = L^2(\mathbb{R}/\mathbb{Z})$:

$$(U\psi)(x) = \psi(x+\alpha), \qquad (V\psi)(x) = \mathrm{e}^{2\pi\mathrm{i}x}\psi(x). \tag{10}$$

The induced classical orbit on the circle is the irrational rotation

$$x_t = x_0 + t\alpha \pmod 1, \tag{11}$$

which is uniquely ergodic and equidistributed [16–19].

3.3 Finite-resolution readout: windows, effects, and induced statistics

Finite-resolution readout is *not* an external sampling axiom; it is part of the protocol. The simplest example is a window $W \subset \mathbb{R}/\mathbb{Z}$ and a binary readout

$$b_t := \mathbf{1}_W(x_t) \in \{0,1\}. \tag{12}$$

More generally, let $\{w_k^{(\varepsilon)}(x)\}_{k\in K}$ be a measurable partition of unity with $w_k^{(\varepsilon)}(x) \in [0,1]$ and $\sum_k w_k^{(\varepsilon)}(x) = 1$. Using the spectral measure Π_V of the phase unitary V, define effects

$$E_k^{(\varepsilon)} := \int_{\mathbb{R}/\mathbb{Z}} w_k^{(\varepsilon)}(x)\,\mathrm{d}\Pi_V(x), \qquad \sum_k E_k^{(\varepsilon)} = \mathbf{1}, \tag{13}$$

and probabilities $P_k^{(\varepsilon)} = \omega_{\mathrm{eff}}(E_k^{(\varepsilon)})$ as in O5.

Theorem 3.3 (Weyl equidistribution and induced frequencies)**.** *If $\alpha \notin \mathbb{Q}$, the orbit $x_t = x_0 + t\alpha \pmod 1$ is equidistributed in $\mathbb{R}/\mathbb{Z}$. In particular, for any interval window W,*

$$\frac{1}{N}\sum_{t=0}^{N-1} \mathbf{1}_W(x_t) \;\longrightarrow\; |W|, \qquad N \to \infty, \tag{14}$$

where $|W|$ is the Lebesgue length of W.

Remark 3.4. *The statement extends to Riemann-integrable functions and, under bounded-variation assumptions, admits explicit finite-N discrepancy bounds; see Section 5. Further details are in Appendix B.5.*

3.4 Symbolic readout and the golden branch

When W is an interval, the binary readout $b_t = \mathbf{1}_W(x_t)$ is a *Sturmian word* (a mechanical word) of minimal complexity $p(n) = n + 1$ [20, 21]. The "golden branch" $\alpha = \varphi^{-1}$ (continued fraction $[0; 1, 1, 1, \dots]$) yields Fibonacci/Sturmian structure and, at the coding interface, the Zeckendorf decomposition. This branch plays the role of a canonical toy sector for explicit bounds (Section 9).

4 The climb: modular flow as renormalization

4.1 Mother space: the modular curve and its cusp interface

Let

$$\mathbb{H} = \{\tau = x + \mathrm{i}y \in \mathbb{C} : \ y > 0\} \tag{15}$$

be the upper half-plane. The modular group $\mathrm{PSL}_2(\mathbb{Z})$ acts by fractional linear transformations

$$\tau \mapsto \frac{a\tau + b}{c\tau + d}, \qquad \begin{pmatrix} a & b \\ c & d \end{pmatrix} \in \mathrm{SL}_2(\mathbb{Z}). \tag{16}$$

The level-1 modular curve is

$$X(1) = \mathrm{PSL}_2(\mathbb{Z}) \backslash (\mathbb{H} \cup \{\text{cusps}\}). \tag{17}$$

It has a single cusp class (see, e.g., [22]). In particular, the inversion $S : \tau \mapsto -1/\tau$ exchanges 0 and ∞ and identifies them in the quotient, providing a canonical "endpoint identification" template (developed further in Section 8).

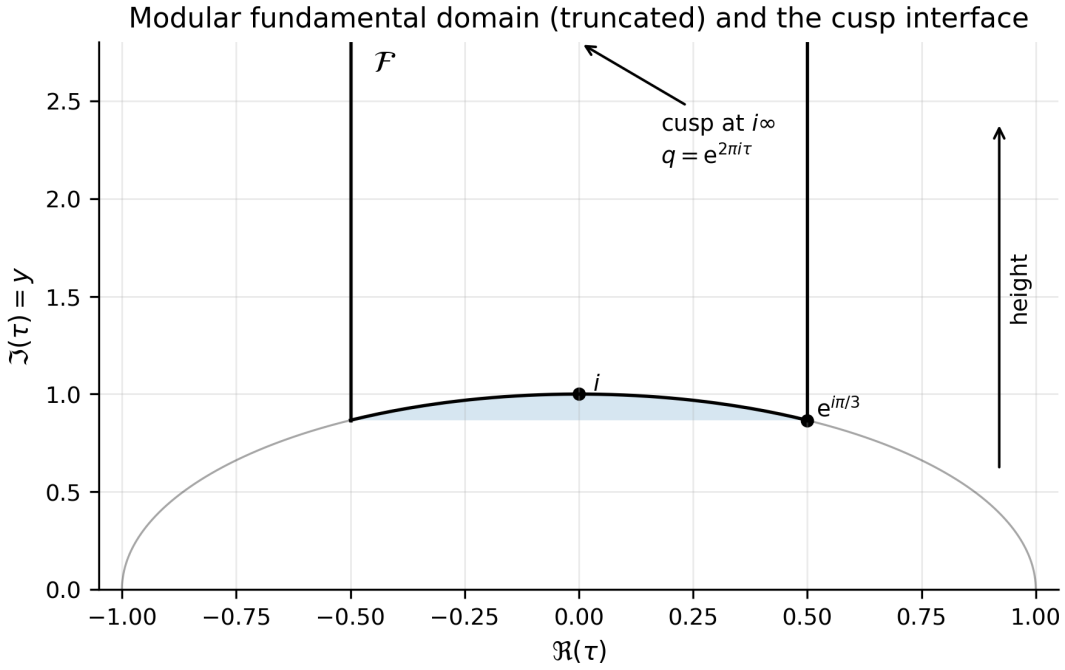

Figure 2: A truncated fundamental domain for $\mathrm{PSL}_2(\mathbb{Z})$ in the upper half-plane, highlighting the cusp direction (height y) and the cusp coordinate $q = \mathrm{e}^{2\pi\mathrm{i}\tau}$ used for discretization at the interface.

Figure 3 gives a protocol-level overview of the stairway: a scan orbit is used to sample a cusp slice, Fourier projection reconstructs coefficients, discrepancy controls finite-N error, and arithmetic constraints (Hecke/Euler) provide auditable closure.

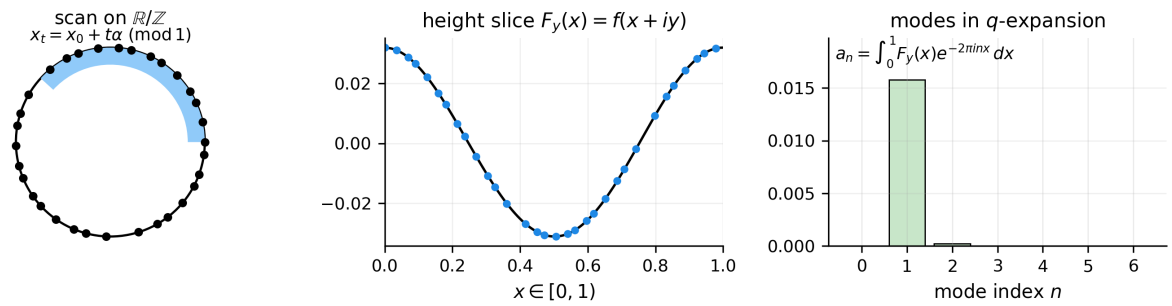

Figure 3: The stairway pipeline as a Layer 1 protocol: scan sampling on the circle provides data, cusp slices provide a continuous-to-discrete interface via Fourier projection, discrepancy provides explicit finite-N control, and arithmetic symmetries (Hecke/Euler) constrain the recovered coefficient spectrum.

4.2 Geodesic flow and the Gauss-map suspension

Define the modular surface

$$M := \mathrm{PSL}_2(\mathbb{Z})\backslash\mathbb{H}. \tag{18}$$

The geodesic flow on the unit tangent bundle T^1M admits a canonical symbolic coding by continued fractions. The key fact, due to Series [13] (see also [17,23]), is that a Poincaré section returns by the Gauss map.

Theorem 4.1 (Series: modular geodesic flow as a Gauss suspension)**.** *There exists a Poincaré section $\Sigma \subset T^1M$ and a measurable isomorphism between $(\Sigma, \text{return map})$ and $((0,1), G)$, where*

$$G(\xi) = \left\{\frac{1}{\xi}\right\} \in (0,1), \qquad \xi \in (0,1), \tag{19}$$

is the Gauss map (fractional part of $1/\xi$). Moreover, the geodesic flow on T^1M is measurably isomorphic to the suspension flow over G with roof function

$$r(\xi) = -2\log\xi. \tag{20}$$

If $\xi = [0; a_1, a_2, \dots]$ is the continued fraction of ξ, then the digit sequence (a_n) is the symbolic orbit of ξ under G.

Scale time. The roof function $r(\xi)$ is additive under suspension concatenation, so the accumulated scale time after n returns is

$$T_n(\xi) = \sum_{j=0}^{n-1} r(G^j\xi) = -2\sum_{j=0}^{n-1} \log(G^j\xi). \tag{21}$$

This makes "climbing in scale" into a computable quantity controlled by the continued-fraction digits.

4.3 Gauss invariant measure and digit laws

The Gauss map preserves the probability measure

$$\mathrm{d}\mu(\xi) = \frac{1}{\log 2}\frac{\mathrm{d}\xi}{1+\xi}, \tag{22}$$

and is ergodic with respect to μ [23]. Consequently, the leading digit $a_1 = \lfloor 1/\xi \rfloor$ has the closed-form law

$$\mu(a_1 = k) = \log_2\left(1 + \frac{1}{k(k+2)}\right), \qquad k \geq 1. \tag{23}$$

A short derivation is given in Appendix B.16.

Metrical constants. Beyond the one-step digit law, metrical continued-fraction theory provides sharp almost-everywhere scaling constants. Examples include Khinchin's constant for geometric means of digits and Lévy's constant for the exponential growth rate of convergent denominators q_n; see [23] for standard statements and proofs. These constants provide additional quantitative rigidity for the "scale time" encoded by continued fractions.

In particular, the Gauss measure expectation of the logarithm has a closed form,

$$\int_0^1 (-\log \xi)\, \mathrm{d}\mu(\xi) = \frac{\pi^2}{12 \log 2}, \tag{24}$$

see Proposition B.16 for a short proof. so the roof function $r(\xi) = -2 \log \xi$ has mean

$$\int_0^1 r(\xi)\, \mathrm{d}\mu(\xi) = \frac{\pi^2}{6 \log 2}. \tag{25}$$

By the ergodic theorem, for μ-almost every ξ,

$$\frac{1}{n} \sum_{j=0}^{n-1} r(G^j \xi) \to \frac{\pi^2}{6 \log 2}, \tag{26}$$

which gives a constant-controlled linear growth law for the accumulated scale time $T_n(\xi)$.

Gauss–Kuzmin convergence (mixing to the Gauss measure). The Gauss map admits an exponential relaxation theorem: for broad classes of absolutely continuous initial distributions, the law of $G^n(\xi)$ converges exponentially fast to the Gauss invariant measure. We treat this as a standard input from metrical continued-fraction theory and do not reprove it here; see [23]. Appendix B.17 records a standard theorem statement.

4.4 From the scan slope to canonical digits: Gauss iteration and Ostrowski coding

The scan protocol is controlled by the irrational slope α in $x_t = x_0 + t\alpha \pmod 1$. The climb acts on the same parameter by Gauss iteration. Write

$$\alpha = [0; a_1, a_2, \dots], \qquad a_n \in \mathbb{N}_{\geq 1}, \tag{27}$$

and define convergents p_n/q_n by the standard continued-fraction recursion. The integer denominators q_n provide canonical "scale blocks" for orbit sums.

The Ostrowski representation theorem states that every $N \in \mathbb{N}$ admits a unique expansion (see, e.g., [23])

$$N = \sum_{n=0}^{m} b_n q_n, \tag{28}$$

where the digits (b_n) satisfy local admissibility constraints determined by the continued-fraction digits (a_n). This representation is a local syntax: admissibility can be checked without global carries.

Golden branch. On the golden branch $\alpha = \varphi^{-1} = [0; 1, 1, 1, \dots]$, Ostrowski coding degenerates to the Zeckendorf decomposition: every integer is uniquely written as a sum of nonconsecutive Fibonacci numbers [24]. This yields a particularly simple binary syntax (no adjacent 1's), and plays the role of a canonical toy sector for explicit bounds and examples.

5 Top interface: cusps, q-expansions, and slice–sampling reconstruction

5.1 Cusps, periodicity, and q-expansions as a canonical continuous–discrete interface

Near the cusp $i\infty$ of the modular curve, a canonical local parameter is

$$q = \mathrm{e}^{2\pi \mathrm{i}\tau}, \qquad \tau = x + \mathrm{i}y. \tag{29}$$

As $y \to \infty$, $|q| = \mathrm{e}^{-2\pi y} \to 0$. For level 1, modular objects are T-invariant ($f(\tau + 1) = f(\tau)$), hence 1-periodic in $x = \Re\tau$ and admit Fourier expansions on each horizontal slice. In particular, any modular form (or more generally, any function analytic at the cusp in the appropriate sense) admits an absolutely convergent Fourier/q-expansion

$$f(\tau) = \sum_{n \geq 0} a_n q^n = \sum_{n \geq 0} a_n \mathrm{e}^{2\pi \mathrm{i} n x} \mathrm{e}^{-2\pi n y}. \tag{30}$$

See, e.g., [22, 25, 26] for standard treatments of q-expansions and cusp Fourier theory. The coefficients (a_n) constitute a discrete integer (or algebraic) spectrum in arithmetic settings; Hecke symmetry then constrains these coefficients rigidly (Section 6).

5.2 A slice–coefficient identity at arbitrary height

The cusp limit $y \to \infty$ is *not* required to recover coefficients. Coefficients can be reconstructed from any height slice by Fourier projection.

Definition 5.1 (height slice)**.** *For any $y > 0$, define the slice function*

$$F_y(x) := f(x + \mathrm{i}y), \qquad x \in [0, 1). \tag{31}$$

Theorem 5.2 (slice–coefficient reconstruction)**.** *Assume that* (30) *converges absolutely and uniformly for fixed $y > 0$. Then for every $n \geq 0$ and every $y > 0$,*

$$a_n = \mathrm{e}^{2\pi n y} \int_0^1 F_y(x)\, \mathrm{e}^{-2\pi \mathrm{i} n x}\, \mathrm{d}x. \tag{32}$$

Proof. By absolute uniform convergence at fixed $y > 0$, we may integrate (30) termwise:

$$\int_0^1 F_y(x)\, \mathrm{e}^{-2\pi \mathrm{i} n x}\, \mathrm{d}x = \sum_{m \geq 0} a_m \mathrm{e}^{-2\pi m y} \int_0^1 \mathrm{e}^{2\pi \mathrm{i}(m-n)x}\, \mathrm{d}x = a_n \mathrm{e}^{-2\pi n y}, \tag{33}$$

since $\int_0^1 \mathrm{e}^{2\pi \mathrm{i}(m-n)x}\, \mathrm{d}x = \delta_{mn}$. Rearranging yields (32). □

Remark 5.3 (when the assumptions hold)**.** *For the holomorphic modular-form objects used in this manuscript, the Fourier coefficients have polynomial growth, hence the q-series converges absolutely and uniformly on every half-strip $\{x \in [0, 1],\, y \geq y_0\}$ for $y_0 > 0$ (Proposition B.8). This justifies termwise integration and differentiation on slices at fixed $y > 0$.*

5.3 Scan-orbit sampling: a finite-N estimator and discrepancy control

We now replace the slice integral by scan-orbit sampling using $x_t = x_0 + t\alpha \pmod 1$ from Axiom O5.

Definition 5.4 (scan-sampled coefficient estimator)**.** *For $n \geq 0$, $y > 0$, and $N \in \mathbb{N}$, define*

$$\widehat{a}_{n,N}(y) := \mathrm{e}^{2\pi n y} \cdot \frac{1}{N} \sum_{t=0}^{N-1} F_y(x_t)\, \mathrm{e}^{-2\pi i n x_t}. \tag{34}$$

To control the approximation error, we use star discrepancy. Given a point set $P_N = \{x_0, \ldots, x_{N-1}\} \subset [0,1)$, define

$$D_N^*(P_N) = \sup_{0 \leq u \leq 1} \left| \frac{1}{N} \sum_{t=0}^{N-1} \mathbf{1}_{[0,u)}(x_t) - u \right|. \tag{35}$$

The Koksma inequality bounds integration error by star discrepancy for bounded-variation functions [19, 27].

Theorem 5.5 (finite-N recovery bound)**.** *Assume $g_{n,y}(x) := F_y(x)\mathrm{e}^{-2\pi i n x}$ has bounded variation on $[0,1]$. Then*

$$|\widehat{a}_{n,N}(y) - a_n| \leq \mathrm{e}^{2\pi n y}\, \mathrm{Var}(g_{n,y})\, D_N^*(P_N). \tag{36}$$

Proof. By Theorem 5.2, $a_n = \mathrm{e}^{2\pi n y} \int_0^1 g_{n,y}(x)\, \mathrm{d}x$. By Koksma's inequality,

$$\left| \frac{1}{N} \sum_{t=0}^{N-1} g_{n,y}(x_t) - \int_0^1 g_{n,y}(x)\, \mathrm{d}x \right| \leq \mathrm{Var}(g_{n,y})\, D_N^*(P_N). \tag{37}$$

Multiplying by $\mathrm{e}^{2\pi n y}$ yields (36). □

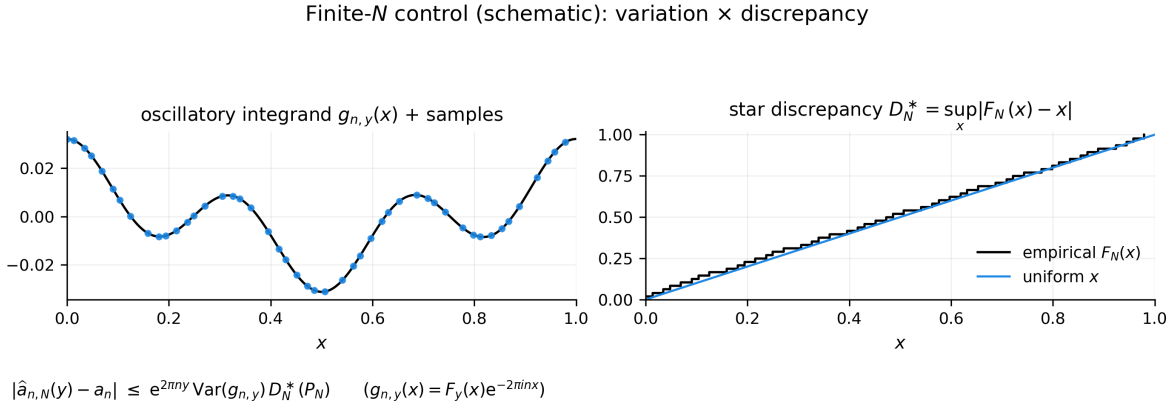

Figure 4: Structure of slice–sampling coefficient recovery: Fourier reconstruction on a fixed height slice, scan-orbit sampling, and an explicit finite-N error bound controlled by variation and star discrepancy (with height dependence carried by $\mathrm{e}^{2\pi n y}$).

Remark 5.6 (complex-valued functions)**.** *The 1D Koksma inequality extends to complex-valued functions with the same constant once* Var *is taken as* $\mathrm{Var}(\Re f) + \mathrm{Var}(\Im f)$ *(Definition B.3). In the modular-form settings considered here, $g_{n,y}$ is absolutely continuous in x at fixed $y > 0$ under standard coefficient-growth assumptions (Appendix B.9), so bounded variation is satisfied.*

Remark 5.7 (explicit variation bounds and end-to-end certification)**.** *For concrete modular objects,* $\mathrm{Var}(g_{n,y})$ *can be bounded with explicit y-dependence; see Appendix B.11–B.12 for closed-form bounds for E_4 and E_6, and Appendix B.8 for a general derivative-based estimate. Theorem 5.5 controls sampling error; a fully certified numerical pipeline additionally requires certified evaluation/truncation and floating-point stability control as a function of (n, y, N) (Appendix D).*

5.4 A period-interface plug: scan averages as integrals, integrals as coefficient data

The slice–sampling estimator makes a structural point explicit: the cusp interface reduces discrete coefficient recovery to the evaluation of an integral on a torus slice, and scan-orbit sampling reduces that integral to a Birkhoff average. This is precisely the bridge isolated and functorialized (in an algebraic subcategory) in the companion period-realization manuscript [28].

A commutative diagram at fixed (n, y). Fix $n \geq 0$ and $y > 0$, and define $g_{n,y}(x) = F_y(x)\mathrm{e}^{-2\pi i n x}$. Then the coefficient identity (32) and the estimator (34) can be summarized as the following commutative limit diagram:

$$\begin{array}{ccc} \frac{1}{N}\sum_{t=0}^{N-1} g_{n,y}(x_t) & \xrightarrow{N\to\infty} & \int_0^1 g_{n,y}(x)\,\mathrm{d}x \\ \big\downarrow \times \mathrm{e}^{2\pi n y} & & \big\downarrow \times \mathrm{e}^{2\pi n y} \\ \widehat{a}_{n,N}(y) & \xrightarrow{N\to\infty} & a_n \end{array}$$

The quantitative content is that finite-N deviation is controlled by a discrepancy/variation bound (Theorem 5.5 and Corollary 5.8).

Relation to periods. The integral on the top-right is an instance of a "readout as an integral" interface. In MAI [28], this interface is made closed and auditable on a controlled protocol subcategory with algebraic (rational) kernels, yielding Kontsevich–Zagier periods as the resulting invariants [29]. In the modular setting, an independent and standard period interface is provided by modular symbols and critical L-values, which are period data up to algebraic factors [30, 31]. The present paper uses the integral only as a coefficient-recovery mechanism; the motivic organization of these period interfaces is recorded as a programmatic target in [28].

5.5 Ostrowski digits and an auditable bound on discrepancy

For irrational rotations, discrepancy admits a digit-auditable upper bound in terms of the Ostrowski expansion (28). In its simplest form, this bound is obtained by combining the Denjoy–Koksma inequality at convergent denominators with an Ostrowski block decomposition; see Appendix B.5.

Corollary 5.8 (Ostrowski digit bound)**.** *Let $N = \sum_{j=0}^{m} b_j q_j$ be the Ostrowski expansion associated with $\alpha = [0; a_1, a_2, \dots]$. Then*

$$D_N^*(P_N) \leq \frac{2}{N}\sum_{j=0}^{m} b_j. \tag{38}$$

Consequently,

$$\left|\widehat{a}_{n,N}(y) - a_n\right| \leq \mathrm{e}^{2\pi n y}\,\mathrm{Var}(g_{n,y}) \cdot \frac{2}{N}\sum_{j=0}^{m} b_j. \tag{39}$$

Remark 5.9 (golden branch / Zeckendorf weight)**.** *On the golden branch $\alpha = \varphi^{-1}$, the Ostrowski expansion degenerates to the Zeckendorf decomposition and $\sum_j b_j$ becomes the Zeckendorf (Fibonacci) Hamming weight $w_Z(N)$, yielding*

$$D_N^*(P_N) \leq \frac{2w_Z(N)}{N}. \tag{40}$$

5.6 Scale trade-offs: smoothing versus amplification

The factor $e^{2\pi ny}$ in (32) and (36) makes a basic numerical truth explicit: increasing y suppresses high-frequency contributions in the slice $F_y(x)$ by $e^{-2\pi ny}$, but recovering the nth coefficient requires multiplication by $e^{2\pi ny}$, which amplifies finite-N sampling error and finite-precision noise. Thus "climbing" is not monotone in "easiness"; rather, the modular scale direction organizes which discrete information is stably accessible at which heights.

This trade-off is already visible in the structure of the reconstruction formula and the finite-N bound.

5.7 Abel radial parameters and the $|q|$ modulus

The cusp modulus satisfies $|q| = e^{-2\pi y} \in (0, 1)$. This is formally analogous to Abel damping parameters used in orbit regularization (Assumption R1): a radial parameter controls how much of a tail is included before taking a limit. In this sense, the q-modulus provides a canonical "radial" coordinate for the cusp interface, compatible with the notion that renormalization consists of separating universal divergences from finite parts when approaching a boundary.

Remark 5.10 (terminology: relation to holographic renormalization)**.** *In the AdS/CFT literature, "holographic renormalization" refers to renormalization via a radial bulk coordinate interpreted as an energy scale, with counterterms and flow equations defined at finite cutoff before taking a boundary limit; see, e.g., [32]. The present paper does not use AdS bulk field equations as an input. We use the term* holographic renormalization-flow *in a protocol sense: the cusp height y (equivalently $|q| = e^{-2\pi y}$) is an intrinsic radial parameter organizing which discrete coefficient data are stably accessible at finite resources, and the "renormalization" step is the auditable passage from finite-resolution readout to discrete arithmetic spectra via slice projection and certified error bounds.*

6 Hecke dynamics: the prime skeleton of the discrete layer

6.1 Hecke operators and their algebraic closure

On spaces of modular forms of level 1 and weight k, Hecke operators T_n form a commutative algebra encoding arithmetic symmetry; standard references include [22, 25]. The defining structure is that Hecke operators are indexed by all $n \geq 1$, but the algebra is generated by the operators at primes.

The fundamental multiplication law is

$$T_m T_n = \sum_{d|(m,n)} d^{k-1}\, T_{mn/d^2}. \tag{41}$$

In particular, if $(m, n) = 1$ then $T_{mn} = T_m T_n$, and for prime powers one obtains the recursion

$$T_{p^{r+1}} = T_p T_{p^r} - p^{k-1} T_{p^{r-1}}, \qquad r \geq 1. \tag{42}$$

6.2 Geometric meaning: Hecke correspondences rescale height

Beyond the abstract algebra, Hecke operators have a concrete geometric action on functions on $\mathbb{H}$ via finite sums of explicit fractional-linear maps (double-coset correspondences). For level 1 holomorphic modular forms of weight k, a standard explicit formula is (see, e.g., [22, 25])

$$(T_n f)(\tau) = n^{k-1} \sum_{\substack{ad=n \\ 0\leq b<d}} d^{-k}\, f\Big(\frac{a\tau + b}{d}\Big) = \sum_{\substack{ad=n \\ 0\leq b<d}} \frac{a^{k-1}}{d}\, f\Big(\frac{a\tau + b}{d}\Big), \tag{43}$$

In particular, for a prime p,

$$(T_p f)(\tau) = p^{k-1} f(p\tau) + \frac{1}{p} \sum_{b=0}^{p-1} f\left(\frac{\tau + b}{p}\right). \tag{44}$$

These maps rescale the slice height $y = \Im\tau$ by rational factors:

$$\Im(p\tau) = p\, y, \qquad \Im\left(\frac{\tau + b}{p}\right) = \frac{y}{p}. \tag{45}$$

Thus primes act as a discrete cross-scale skeleton: one term pushes deeper into the cusp ($y \mapsto py$) while the other pulls back toward the boundary ($y \mapsto y/p$).

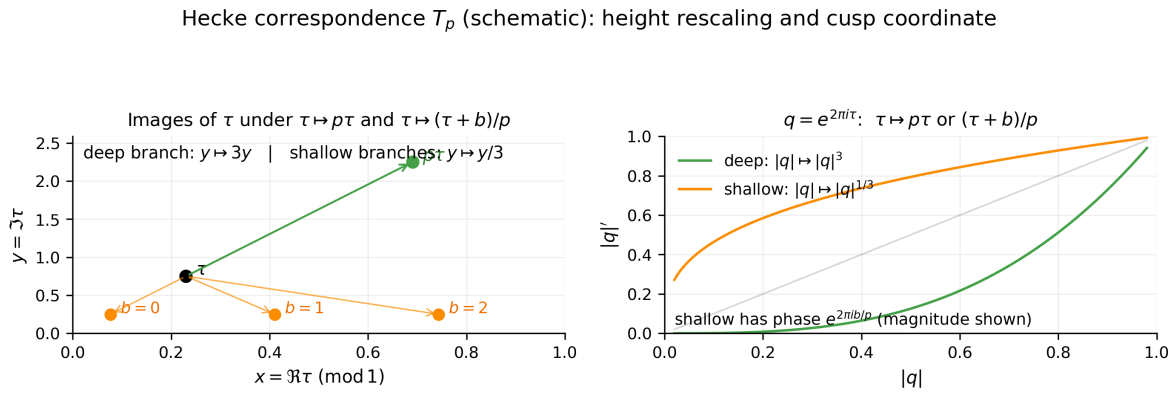

Figure 5: Hecke correspondence for a prime p (schematic): the explicit formula is a finite sum over fractional-linear maps, with branches that rescale the slice height by $y \mapsto py$ and $y \mapsto y/p$. In the full sum, the action closes on integer-indexed q-expansion coefficients.

Remark 6.1 (action on the cusp coordinate)**.** *Under $\tau \mapsto p\tau$ one has $q \mapsto q^p$. Under $\tau \mapsto (\tau + b)/p$, one has $q \mapsto e^{2\pi ib/p}\, q^{1/p}$. In the full Hecke sum (44) the fractional powers cancel, and T_p preserves the usual q-expansion space, which is another way to see why the prime skeleton closes on integer-indexed coefficients.*

6.3 From double cosets to q-coefficients (explicit closure)

The statement that "fractional powers cancel" can be made completely explicit at the coefficient level.

Proposition 6.2 (Hecke action on Fourier coefficients)**.** *Let f be a holomorphic modular form of weight k with q-expansion*

$$f(\tau) = \sum_{m \geq 0} a_m q^m, \qquad q = e^{2\pi i\tau}. \tag{46}$$

Then $T_n f$ has the q-expansion

$$(T_n f)(\tau) = \sum_{\ell \geq 0} \left(\sum_{d \mid (n,\ell)} d^{k-1}\, a_{n\ell/d^2} \right) q^\ell. \tag{47}$$

In particular, for a prime p,

$$(T_p f)(\tau) = \sum_{\ell \geq 0} \left(a_{p\ell} + p^{k-1} a_{\ell/p} \right) q^\ell, \tag{48}$$

where $a_{\ell/p} = 0$ if $p \nmid \ell$.

Proof. Insert the q-expansion of f into the explicit formula (43) and use the root-of-unity sum

$$\sum_{b=0}^{d-1} \mathrm{e}^{2\pi i m b/d} = \begin{cases} d, & d \mid m, \\ 0, & d \nmid m. \end{cases} \tag{49}$$

Writing $m = dm'$ and collecting coefficients of q^ℓ yields the stated divisor sum; see [22, 25] for standard derivations. □

6.4 Protocol-level meaning of T_p: a testable prime-skeleton check

The formal action of T_p on modular observables is completely explicit (Equation (44)) and induces a closed coefficient-level map (Proposition 6.2). For the present paper's protocol chain, it is useful to separate two notions of "Hecke acting on the protocol".

(i) Coefficient-layer closure (used here). Once a coefficient sequence (a_n) is recovered (with a certified error budget) from slice sampling, the prime skeleton supplies a *locally checkable* constraint family. For a prime p, define the induced operator on coefficient sequences by

$$(\mathcal{T}_p a)_\ell := a_{p\ell} + p^{k-1} a_{\ell/p}, \qquad a_{\ell/p} := 0 \text{ if } p \nmid \ell. \tag{50}$$

Then $T_p f$ has coefficients $\mathcal{T}_p a$. If f is a normalized Hecke eigenform, the eigen-relation $T_p f = a_p f$ becomes the coefficient identity

$$\mathcal{T}_p a = a_p\, a, \tag{51}$$

which is an explicit prime-indexed consistency test on the recovered discrete spectrum.

Remark 6.3 (normalization convention)**.** *Throughout, "normalized Hecke eigenform" means the standard normalization $a_1 = 1$ in the q-expansion. For an eigenform scaled by a nonzero constant, one can always renormalize by dividing the coefficient sequence by a_1 before applying the prime-skeleton identities.*

(ii) Implementable channel on instruments (additional structure). Interpreting T_p as a physical symmetry acting within a fixed effective observer sector $\mathcal{H}_{\text{eff}}$ requires an explicit interface that maps a modular observable f to an operator-valued readout observable and that can realize the branch mixing $\tau \mapsto p\tau$ and $\tau \mapsto (\tau + b)/p$ operationally. This is naturally cross-scale (it mixes heights $y \mapsto py$ and $y \mapsto y/p$), and therefore goes beyond the coefficient-level closure used in this paper. A fully worked finite-resolution model and a discussion of this distinction are recorded in Appendix C.3.

6.5 Quantitative Hecke consistency under certified coefficient errors

The prime-skeleton constraints are most useful when they can be evaluated with a certified tolerance implied by the coefficient-recovery error budgets. We record a simple deterministic residual bound showing how coefficient-level uncertainty propagates into Hecke-eigen consistency checks.

Definition 6.4 (Hecke residual at a prime)**.** *Fix a weight k and a prime p. For a candidate coefficient sequence $b = (b_n)_{n\ge 1}$, define the residual*

$$R_{p,\ell}(b) := (b_{p\ell} + p^{k-1} b_{\ell/p}) - b_p b_\ell, \qquad b_{\ell/p} := 0 \text{ if } p \nmid \ell. \tag{52}$$

Remark 6.5. *The residual* (52) *tests the normalized Hecke-eigen identity. If one starts from an unnormalized coefficient sequence a with $a_1 \neq 0$, apply it to $b_n := a_n/a_1$.*

Proposition 6.6 (residual bound from coefficient error bars)**.** *Assume f is a normalized Hecke eigenform so that its true coefficients satisfy*

$$a_{p\ell} + p^{k-1} a_{\ell/p} = a_p a_\ell \qquad (\ell \geq 1),$$

where $a_{\ell/p} := 0$ if $p \nmid \ell$, and let $\widehat{a}$ be an approximate coefficient sequence. Suppose for a given pair (p, ℓ) we have certified bounds

$$|\widehat{a}_m - a_m| \leq \delta_m \qquad \text{for } m \in \{p\ell,\ p,\ \ell\} \text{ and also for } m = \ell/p \text{ when } p \mid \ell,$$

with the convention $\delta_{\ell/p} := 0$ if $p \nmid \ell$. Then the Hecke residual satisfies

$$|R_{p,\ell}(\widehat{a})| \leq \delta_{p\ell} + p^{k-1}\delta_{\ell/p} + |a_p|\delta_\ell + |a_\ell|\delta_p + \delta_p\delta_\ell. \tag{53}$$

Proof. Insert the true identity $a_{p\ell} + p^{k-1}a_{\ell/p} = a_p a_\ell$ into Definition 6.4:

$$R_{p,\ell}(\widehat{a}) = (\widehat{a}_{p\ell} - a_{p\ell}) + p^{k-1}(\widehat{a}_{\ell/p} - a_{\ell/p}) - (\widehat{a}_p\widehat{a}_\ell - a_p a_\ell).$$

For the product term,

$$\widehat{a}_p\widehat{a}_\ell - a_p a_\ell = (\widehat{a}_p - a_p)\widehat{a}_\ell + a_p(\widehat{a}_\ell - a_\ell),$$

so $|\widehat{a}_p\widehat{a}_\ell - a_p a_\ell| \leq \delta_p(|a_\ell| + \delta_\ell) + |a_p|\delta_\ell$. Combining these inequalities yields (53). □

Remark 6.7 (turning residual bounds into falsifiable fits)**.** *In arithmetic settings, $|a_p|$ admits explicit majorants (e.g. Deligne/Ramanujan–Petersson for cuspidal eigenforms; see, e.g., [22, 26, 33]), so* (53) *becomes a fully explicit, deterministic tolerance for a Hecke-eigen "fit" test. In the special case where $a_n \in \mathbb{Z}$ and coefficients are recovered exactly by rounding (Corollary 9.5), the residual vanishes identically: $R_{p,\ell}(\widehat{a}) = 0$ for all tested primes and indices.*

6.6 Eigenforms: stable directions and coefficient rigidity

If f is a normalized Hecke eigenform with q-expansion

$$f(\tau) = \sum_{n \geq 1} a_n q^n, \tag{54}$$

then

$$T_n f = a_n f, \tag{55}$$

so the q-coefficients coincide with Hecke eigenvalues (up to normalization conventions). The Hecke relations immediately imply two rigid constraints on the coefficient spectrum:

1. **Coprime multiplicativity.** If $(m, n) = 1$, then

$$a_{mn} = a_m a_n. \tag{56}$$

2. **Prime-power recursion.** For any prime p and $r \geq 1$,

$$a_{p^{r+1}} = a_p a_{p^r} - p^{k-1} a_{p^{r-1}}. \tag{57}$$

Thus the discrete spectrum is not an arbitrary integer sequence: it is generated and constrained by the prime skeleton.

6.7 Example: Ramanujan's discriminant and $\tau(n)$

The classical example is the weight-12 cusp form

$$\Delta(\tau) = q \prod_{n \geq 1} (1 - q^n)^{24} = \sum_{n \geq 1} \tau(n) q^n, \tag{58}$$

whose coefficients $\tau(n)$ satisfy the Hecke constraints above (with $k = 12$). These relations provide a canonical instance of the prime-generated skeleton at the coefficient level.

6.8 Euler products and local-to-global closure

For normalized eigenforms, the Dirichlet series

$$L(s,f) = \sum_{n\geq 1} \frac{a_n}{n^s} \tag{59}$$

admits an Euler product factorization

$$L(s,f) = \prod_p \left(1 - a_p p^{-s} + p^{k-1} p^{-2s}\right)^{-1}. \tag{60}$$

This expresses local-to-global closure explicitly: prime-indexed data determine the full spectrum.

7 Langlands semantics: from Hecke spectra to Galois "source code"

Up to this point, the chain

$$\begin{aligned} &\text{scan algebra } A_\alpha \\ &\Longrightarrow \text{ modular renormalization flow} \\ &\Longrightarrow \ q\text{-expansion coefficients} \\ &\Longrightarrow \text{ Hecke prime skeleton} \end{aligned} \tag{61}$$

is closed within Layer 0/1 mathematics. This section provides an organizational semantics for the same integer spectra and is not used as a premise in any Layer 0/1 derivation. The Langlands program reinterprets Hecke eigenvalues as automorphic parameters and, in suitable settings, as traces of Frobenius under Galois representations.

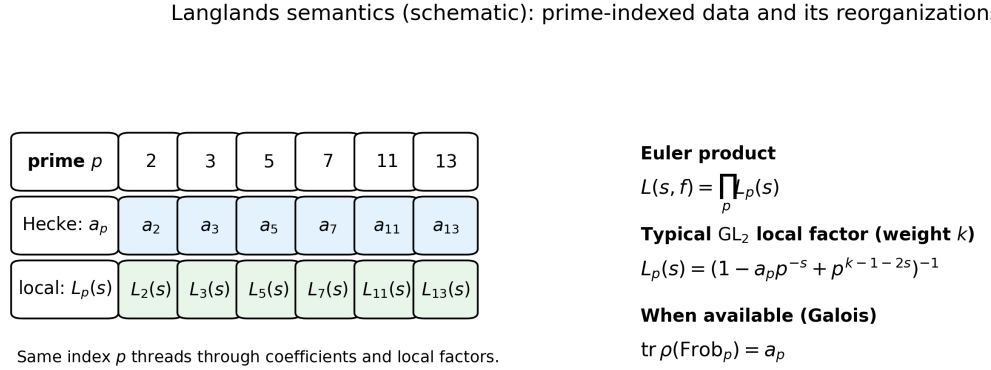

Figure 6: A schematic Langlands pipeline: the same prime-indexed Hecke spectrum can be packaged as automorphic local parameters and, when available, as traces of Frobenius under an attached Galois representation.

7.1 From modular forms to automorphic representations

For $GL_2/\mathbb{Q}$, a normalized Hecke eigen cusp form f corresponds to an automorphic representation π_f of $\mathrm{GL}_2(\mathbb{A}_\mathbb{Q})$, with local parameters (Satake parameters) determined by the Hecke eigenvalues a_p at almost all primes. The associated L-function

$$L(s,f) = \sum_{n\geq 1} \frac{a_n}{n^s} = \prod_p \left(1 - a_p p^{-s} + p^{k-1} p^{-2s}\right)^{-1} \tag{62}$$

is therefore an automorphic object encoding the full Hecke spectrum; see, e.g., [34] for standard background on automorphic representations and Hecke parameters.

7.2 Galois representations: making primes into operators

For suitable eigenforms (e.g. newforms), one can attach an ℓ-adic Galois representation

$$\rho_f : \mathrm{Gal}(\overline{\mathbb{Q}}/\mathbb{Q}) \to \mathrm{GL}_2(\overline{\mathbb{Q}}_\ell), \tag{63}$$

such that for almost all primes p,

$$\operatorname{tr} \rho_f(\mathrm{Frob}_p) = a_p, \qquad \det \rho_f(\mathrm{Frob}_p) = p^{k-1}. \tag{64}$$

In this sense, the visible Hecke spectrum is a projection of a deeper symmetry action carried by $\mathrm{Gal}(\overline{\mathbb{Q}}/\mathbb{Q})$ (see, e.g., [26, 35, 36] for standard accounts).

7.3 A programmatic extension: a holographic Langlands functor

The "stairway" viewpoint suggests a natural organizational target: promote the closed GL_2 chain to a functorial construction across a broader class of symmetry groups. We record this as a programmatic definition goal.

Definition 7.1 (Holographic Langlands functor (working definition))**.** *Let* Scan *be a category of scan–readout protocols. An object is a triple*

$$(\, A_\alpha,\ \omega_{\mathrm{eff}},\ \mathcal{I}^{(\varepsilon)} \,), \tag{65}$$

where A_α is the rotation algebra, ω_{eff} is an effective state, and $\mathcal{I}^{(\varepsilon)}$ is a finite-resolution instrument (a family of effects and post-measurement updates) at resolution ε. Morphisms are equivalences preserving the Weyl structure and readout statistics (e.g. implemented by Morita equivalence together with state pullback, under appropriate interface conditions).

Let $\mathsf{AutRep}(G)$ *denote an appropriate category of automorphic representations for a reductive group G. We seek a functor*

$$\mathcal{HL} : \mathsf{Scan} \to \mathsf{AutRep}(G) \tag{66}$$

such that:

- *a renormalization flow (Gauss/geodesic flow) on* Scan *is sent to a natural Hecke/parameter flow on* $\mathsf{AutRep}(G)$*;*
- *cusp discretization and its coefficient spectrum correspond to Hecke eigenvalues in the image;*
- *prime-generated closure on the coefficient side corresponds to Euler-product factorization on the automorphic side.*

Remark 7.2. *Definition 7.1 is not used as a premise in any derivation in this paper. It is a clean mathematical task statement: to turn the closed GL_2 toy chain into a functorial framework that can, in principle, be lifted to general G.*

8 S-inversion as scale exchange and algebraic equivalence

8.1 Modular inversion and cusp endpoint identification

The modular group is generated by

$$T : \tau \mapsto \tau + 1, \qquad S : \tau \mapsto -\frac{1}{\tau}. \tag{67}$$

On the modular curve $X(1)$, the cusp orbit is unique, so $0 \sim \infty$ in the quotient. The inversion S exchanges these endpoints and therefore provides a strict mathematical template for "deep/shallow" identification.

Explicitly, for $\tau = x + \mathrm{i}y$,

$$S(\tau) = -\frac{1}{\tau} = -\frac{x - \mathrm{i}y}{x^2 + y^2}, \qquad \Im S(\tau) = \frac{y}{x^2 + y^2}. \tag{68}$$

Thus, when x is not large, y is exchanged with $1/y$ at the level of scale magnitude: large height and small height are directly related by S.

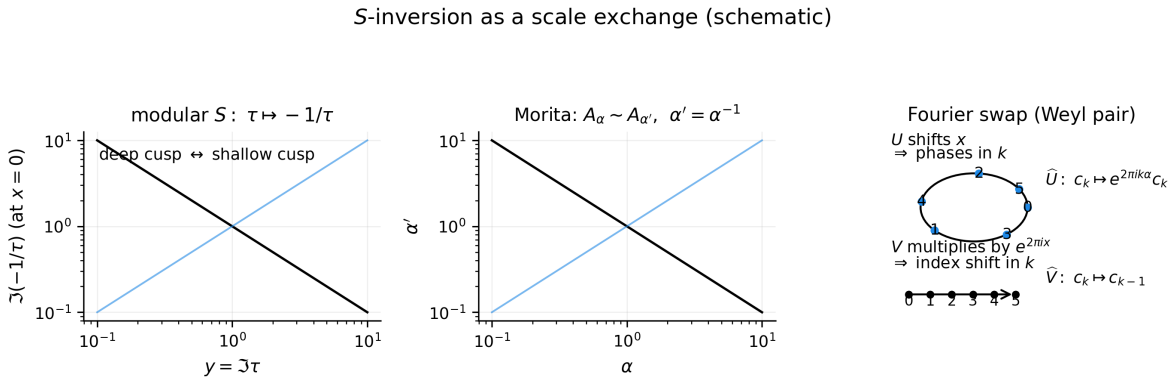

Figure 7: Schematic view of scale exchange: modular S-inversion relates deep and shallow cusp regions; on noncommutative tori, the corresponding $\mathrm{SL}_2(\mathbb{Z})$ action implements Morita equivalence of slope parameters; Fourier exchange swaps scan and readout roles in the covariant Weyl pair.

8.2 Morita equivalence of noncommutative tori and the $\mathrm{SL}_2(\mathbb{Z})$ action

Noncommutative tori admit a canonical $\mathrm{SL}_2(\mathbb{Z})$ action on the slope parameter:

$$\alpha' = \frac{a\alpha + b}{c\alpha + d}, \qquad \gamma = \begin{pmatrix} a & b \\ c & d \end{pmatrix} \in \mathrm{SL}_2(\mathbb{Z}). \tag{69}$$

A foundational result is that A_α and $A_{\alpha'}$ are Morita equivalent (and therefore represent the same "noncommutative geometry" up to equivalence of module categories) [14, 15, 37].

Theorem 8.1 (Morita equivalence classification (standard))**.** *For irrational parameters $\alpha, \beta \in \mathbb{R} \setminus \mathbb{Q}$, the noncommutative tori A_α and A_β are (strongly) Morita equivalent if and only if there exists $\gamma = \begin{pmatrix} a & b \\ c & d \end{pmatrix} \in \mathrm{SL}_2(\mathbb{Z})$ such that*

$$\beta = \frac{a\alpha + b}{c\alpha + d}. \tag{70}$$

Remark 8.2. *See [15, 37] for proofs and further structure (projective modules and K-theory invariants).*

In particular, the modular inversion

$$S = \begin{pmatrix} 0 & -1 \\ 1 & 0 \end{pmatrix} \tag{71}$$

acts by $\alpha \mapsto -1/\alpha$, which is structurally aligned with the Gauss-map inversion step underlying continued fractions.

8.3 Fourier exchange: swapping scan and readout roles

In the covariant representation (10), the Fourier transform exchanges translation and multiplication. Abstractly, this realizes a "scan–readout swap": in one representation, U acts as a tick shift and V acts as a phase; in the Fourier-dual representation, these roles are interchanged.

Proposition 8.3 (Fourier exchange for the covariant Weyl pair)**.** *Let U, V act on $\mathcal{H} = L^2(\mathbb{R}/\mathbb{Z})$ by $(U\psi)(x) = \psi(x+\alpha)$ and $(V\psi)(x) = \mathrm{e}^{2\pi \mathrm{i} x}\psi(x)$ as in (10). Let $\mathcal{F} : \mathcal{H} \to \ell^2(\mathbb{Z})$ be the Fourier transform*

$$(\mathcal{F}\psi)(k) = \int_0^1 \psi(x)\, \mathrm{e}^{-2\pi \mathrm{i} k x}\, \mathrm{d}x. \tag{72}$$

Then on $\ell^2(\mathbb{Z})$ one has

$$\mathcal{F}U\mathcal{F}^{-1} : \widehat{\psi}(k) \mapsto \mathrm{e}^{2\pi \mathrm{i} k\alpha}\widehat{\psi}(k), \qquad \mathcal{F}V\mathcal{F}^{-1} : \widehat{\psi}(k) \mapsto \widehat{\psi}(k-1). \tag{73}$$

In particular, translation (scan shift) becomes phase multiplication in Fourier space, while phase multiplication becomes an index shift, realizing a concrete scan–readout exchange.

Proof. For the first identity, compute

$$(\mathcal{F}U\psi)(k) = \int_0^1 \psi(x+\alpha)\mathrm{e}^{-2\pi \mathrm{i} k x}\, \mathrm{d}x = \mathrm{e}^{2\pi \mathrm{i} k\alpha}\int_0^1 \psi(u)\mathrm{e}^{-2\pi \mathrm{i} k u}\, \mathrm{d}u = \mathrm{e}^{2\pi \mathrm{i} k\alpha}(\mathcal{F}\psi)(k), \tag{74}$$

using the substitution $u = x + \alpha$ and periodicity on $\mathbb{R}/\mathbb{Z}$. The second identity follows similarly:

$$(\mathcal{F}V\psi)(k) = \int_0^1 \mathrm{e}^{2\pi \mathrm{i} x}\psi(x)\mathrm{e}^{-2\pi \mathrm{i} k x}\, \mathrm{d}x = \int_0^1 \psi(x)\mathrm{e}^{-2\pi \mathrm{i}(k-1)x}\, \mathrm{d}x = (\mathcal{F}\psi)(k-1). \tag{75}$$

□

Remark 8.4 (interpretation-layer language)**.** *It is tempting to interpret S and Morita/Fourier equivalence as a "scale-exchange wormhole" that short-circuits intermediate scales. Such language is Layer 2 semantics. The Layer 0/1 content used here is strictly the symmetry/equivalence structure: cusp endpoint identification on $X(1)$ and Morita/Fourier exchange on A_α.*

9 Quantitative closure: explicit bounds at finite resolution

As a closed argument, the stairway chain relies on theorem-level quantitative statements that remain valid at finite resolution and finite tick length. This section collects the bounds used in later arguments.

9.1 Finite-N readout error and discrepancy

On an irrational rotation orbit, Weyl equidistribution implies induced Lebesgue measure (Theorem 3.3). For an interval-window readout, finite-N deviation is controlled by star discrepancy via the Koksma inequality (Appendix B.3). Ostrowski digit bounds then control discrepancy in terms of a locally checkable digit sum (Appendix B.5).

9.2 Slice–coefficient reconstruction and a finite-N coefficient bound

At the cusp interface, Fourier projection gives a height-slice coefficient reconstruction identity (Theorem 5.2). Under scan-orbit sampling, the finite-N estimator admits an explicit discrepancy-controlled bound (Theorem 5.5). The dependence on height y is governed by the factor $\mathrm{e}^{2\pi n y}$, making the smoothing/amplification trade-off explicit.

9.3 Finite-alphabet readout: sampling + quantization and exact integer recovery

The bounds above control only the *sampling* deviation of an orbit average from a slice integral. To close the protocol at finite resolution, one must also account for the fact that a finite-alphabet instrument does not return the exact phase $x_t \in \mathbb{R}/\mathbb{Z}$, but only a representative $\widetilde{x}_t$ with a controlled quantization error.

Definition 9.1 (quantized scan-sampled coefficient estimator)**.** *Fix $n \geq 0$ and $y > 0$, and let $g_{n,y}(x) = f(x + \mathrm{i}y)\,\mathrm{e}^{-2\pi\mathrm{i}nx}$ as in Section 5. Let $x_t = x_0 + t\alpha \pmod 1$ be the underlying scan orbit and suppose the readout returns $\widetilde{x}_t \in [0,1)$ satisfying*

$$|x_t - \widetilde{x}_t| \leq \frac{\varepsilon}{2} \qquad (t = 0, \ldots, N-1). \tag{76}$$

Define the quantized estimator

$$\widehat{a}^{(\varepsilon)}_{n,N}(y) := \mathrm{e}^{2\pi ny} \cdot \frac{1}{N} \sum_{t=0}^{N-1} g_{n,y}(\widetilde{x}_t). \tag{77}$$

Theorem 9.2 (finite-alphabet recovery bound (sampling + quantization))**.** *Assume $g_{n,y}$ is absolutely continuous on $[0,1]$ and has essentially bounded derivative $\|g'_{n,y}\|_\infty < \infty$. Let $P_N = \{x_0, \ldots, x_{N-1}\}$ be the underlying (unquantized) orbit point set. Then*

$$|\widehat{a}^{(\varepsilon)}_{n,N}(y) - a_n| \leq \mathrm{e}^{2\pi ny} \left(\mathrm{Var}(g_{n,y})\, D^*_N(P_N) \;+\; \frac{\varepsilon}{2}\, \|g'_{n,y}\|_\infty \right). \tag{78}$$

Proof. Write

$$\frac{1}{N} \sum_{t=0}^{N-1} g_{n,y}(\widetilde{x}_t) - \int_0^1 g_{n,y} = \left(\frac{1}{N} \sum_{t=0}^{N-1} g_{n,y}(x_t) - \int_0^1 g_{n,y} \right) \;+\; \frac{1}{N} \sum_{t=0}^{N-1} \big(g_{n,y}(\widetilde{x}_t) - g_{n,y}(x_t) \big).$$

The first term is bounded by $\mathrm{Var}(g_{n,y}) D^*_N(P_N)$ by Koksma's inequality (Theorem B.4). For the second term, the assumption $\|g'_{n,y}\|_\infty < \infty$ implies the uniform Lipschitz bound $|g_{n,y}(\widetilde{x}) - g_{n,y}(x)| \leq \|g'_{n,y}\|_\infty |\widetilde{x} - x|$, and (76) gives $|\widetilde{x}_t - x_t| \leq \varepsilon/2$. Multiplying by $\mathrm{e}^{2\pi ny}$ yields (78). □

Remark 9.3 (regularity of the sliced integrand)**.** *For the modular-form observables used in this manuscript, Proposition B.8 implies that $F_y(x) = f(x + \mathrm{i}y)$ is C^1 in x for every fixed $y > 0$ (by termwise differentiation under uniform absolute convergence on half-strips). Hence $g_{n,y}(x) = F_y(x)\mathrm{e}^{-2\pi\mathrm{i}nx}$ has bounded derivative on $[0,1]$, so the assumption $\|g'_{n,y}\|_\infty < \infty$ in Theorem 9.2 is satisfied in the intended arithmetic examples.*

Remark 9.4 (adding certified evaluation/truncation error)**.** *If $F_y(\widetilde{x}_t) = f(\widetilde{x}_t + \mathrm{i}y)$ is computed numerically (e.g. by truncating a q-expansion), then an additional explicit evaluation error term can be added to* (78)*. For Eisenstein series, Appendix B.13 provides closed-form tail bounds at fixed $|q| = \mathrm{e}^{-2\pi y}$.*

Corollary 9.5 (exact integer recovery by rounding)**.** *Let $f(\tau) = \sum_{n \geq 0} a_n q^n$ have integer coefficients $a_n \in \mathbb{Z}$. If the right-hand side of* (78) *is $< \frac{1}{2}$, then rounding $\widehat{a}^{(\varepsilon)}_{n,N}(y)$ to the nearest integer recovers a_n exactly.*

Proof. If $|\widehat{a} - a_n| < 1/2$ and $a_n \in \mathbb{Z}$, the nearest-integer map is unique and equals a_n. □

9.4 Parameter choices: convergent lengths and constant-type slopes

The bounds above become fully explicit once $D_N^*(P_N)$ is controlled in terms of the continued-fraction digits of α. Two robust, auditable choices are:

- **Convergent-length sampling.** If p/q satisfies $0 < |\alpha - p/q| < 1/q^2$ and $N = q$, then Proposition B.7 gives an explicit closed form for $D_q^*(P_q(\alpha))$, implying in particular $D_N^*(P_N) \le 2/N$.
- **Constant-type slopes.** If $\alpha = [0; a_1, a_2, \ldots]$ has bounded partial quotients $a_j \le A$, then Appendix B.5 gives
$$D_N^*(P_N) \le \frac{2A(2 + \log_\varphi N)}{N},$$
providing an explicit $O((\log N)/N)$ rate with auditable constants.

9.5 Truncation control for modular objects

When modular forms are evaluated via truncated q-series, explicit tail bounds provide certified truncation budgets (Appendix B.13). These bounds can be propagated through algebraic identities, such as $j = 1728E_4^3/(E_4^3 - E_6^2)$, to obtain certified error budgets at fixed τ.

10 Conclusion and open problems

We proposed a *holographic renormalization-flow* view of the continuous–discrete bridge: not only a static list of objects (scan algebra, modular curve, cusp coefficients, Hecke operators), but an explicit *climb* that is computable and auditable. The closed Layer 0/1 chain can be summarized as:

$$\begin{aligned} &\text{Weyl pair} \Rightarrow A_\alpha \\ &\Rightarrow \text{(modular) geodesic/Gauss flow} \\ &\Rightarrow \text{continued-fraction digits and Ostrowski syntax} \\ &\Rightarrow q\text{-expansion coefficients at the cusp} \\ &\Rightarrow \text{Hecke prime skeleton.} \end{aligned} \tag{79}$$

Within this chain, the slice–sampling identity and the coefficient estimators make "how integers are extracted from analytic data" into a quantitative pipeline with explicit error controls. At finite alphabet resolution, Theorem 9.2 provides a deterministic sampling+quantization error budget, and Corollary 9.5 gives an exact integer-recovery-by-rounding criterion when $a_n \in \mathbb{Z}$. Once coefficients are recovered (exactly, or with certified error bars), the prime skeleton supplies a falsifiable consistency layer: Hecke-eigen consistency can be tested by the residual bound in Proposition 6.6. Appendix C.2.4 records a fully explicit numerical instance of certified exact recovery for E_4. More generally, the level-1 valence formula implies finite determination of a weight-k modular form by finitely many initial q-coefficients (Appendix B.2), turning finite coefficient recovery into a finite-dimensional identification/fit problem.

We also recorded a strict symmetry template for scale exchange: the modular S-inversion identifies cusp endpoints on $X(1)$ and exchanges deep/shallow regimes; on the noncommutative side, the corresponding $\mathrm{SL}_2(\mathbb{Z})$ action appears via Morita equivalence and Fourier exchange. Interpretation-layer narratives ("wormholes" or "UV/IR shortcuts") are not used as premises.

Open problems. The present paper deliberately isolates tasks that are mathematically well-posed and audit-friendly.

- **Functorial upgrade.** Make Definition 7.1 precise on a controlled subcategory of protocols and prove functoriality (at least for a GL_2 toy class).

- **Protocol equivalence criteria.** Give sharp, checkable conditions under which two scan–readout protocols yield the same observable statistics (e.g. via Morita equivalence and state/instrument compatibility).
- **Certified error budgets.** Extend the discrepancy-based bounds to certified numerical error budgets for coefficient recovery at finite height and finite resolution (truncation, floating-point, instrument noise), and identify scale windows optimizing condition numbers for specific coefficients.
- **Data-to-spectrum interfaces.** Formalize how the discrete coefficient spectrum constrained by Hecke dynamics is linked to any externally specified observable spectrum, while maintaining the layer discipline.
- **Factoring through period data.** A controlled "motive-at-infinity" interface [28] suggests splitting the functorial upgrade into an auditable first arrow from protocols to period data (scan averages as integrals), followed by a programmatic period-to-motive-to-ětale/automorphic factorization:

$$\mathsf{Scan}_{\mathrm{alg}} \to \mathsf{PerDatum} \to (\mathsf{Motives}) \to (\mathsf{GalRep/AutRep}).$$

  The first arrow can be closed on a controlled protocol class; the remaining arrows are the locus of genuinely motivic/Langlands input.

A Audit table: stratification and dependency chain

A.1 Stratification discipline

- **Layer 0:** states and algebras only (Axioms O1–O4).
- **Layer 1:** scan–projection protocols, finite-resolution instruments, induced statistics, and the modular renormalization flow object (Axioms O5–O6 and the mother-space choice in Section 2.3).
- **Layer 2:** semantic interpretation (UV/IR, wormholes, physical spectra) as optional commentary. Layer 2 is never used as a premise.

A.2 Dependency chain (closed part)

The closed, auditable dependency chain of the paper is:

1. O5/O6 $\Rightarrow$ irrational rotation scan $x_t = x_0 + t\alpha \pmod 1$ and induced measure (Theorem 3.3).
2. Modular surface geodesic flow $\Rightarrow$ Gauss-map suspension $\Rightarrow$ continued-fraction digit law (Theorem 4.1 and (23)).
3. Continued fractions $\Rightarrow$ Ostrowski coding of tick length N as a locally auditable digit string (Section 4.4).
4. Cusp interface $q = \mathrm{e}^{2\pi \mathrm{i} \tau}$ $\Rightarrow$ discrete coefficient spectrum via q-expansion (Section 5.1).
5. Slice–coefficient identity and scan sampling $\Rightarrow$ finite-N coefficient estimator with discrepancy/Ostrowski error control (Theorem 5.5 and Corollary 5.8).
6. Hecke relations $\Rightarrow$ prime-generated skeleton constraining coefficient spectra (Section 6).

A.3 Status classification

- **Axioms/definitions:** O1–O6, R1; protocol/slice definitions.
- **Standard theorems:** Weyl equidistribution, Series coding, Gauss invariant measure, Koksma and Denjoy–Koksma inequalities, Hecke relations.
- **Programmatic targets:** holographic Langlands functor (Definition 7.1) and protocol equivalence criteria.

B Mathematical notes and auxiliary lemmas

B.1 Hecke prime-power recursion and prime generation

Starting from the Hecke multiplication relation (41), take $m = p^r$ and $n = p$ for a prime p. The divisors of (p^r, p) are $d \in \{1, p\}$, so

$$T_{p^r} T_p = \sum_{d|(p^r,p)} d^{k-1} T_{p^{r+1}/d^2} = T_{p^{r+1}} + p^{k-1} T_{p^{r-1}}. \tag{80}$$

Rearranging gives the prime-power recursion (42):

$$T_{p^{r+1}} = T_p T_{p^r} - p^{k-1} T_{p^{r-1}}. \tag{81}$$

This shows that all T_{p^r} are generated by T_p. Together with (41) and coprime multiplicativity, it implies that the full Hecke algebra is generated by $\{T_p\}_{p \text{ prime}}$.

B.2 Valence formula and finite determination by cusp coefficients

The modular curve $X(1) = \mathrm{PSL}_2(\mathbb{Z})\backslash(\mathbb{H} \cup \{\text{cusps}\})$ has a single cusp at ∞, so the q-expansion at $i\infty$ encodes the order of vanishing at the cusp. A standard rigidity input is the valence formula for level 1 modular forms; see, e.g., [22, 25, 26].

Theorem B.1 (valence formula on $\mathrm{SL}_2(\mathbb{Z})$ (standard))**.** *Let f be a nonzero holomorphic modular form of weight k on $\mathrm{SL}_2(\mathbb{Z})$, and let $\rho = \mathrm{e}^{2\pi \mathrm{i}/3}$. Then*

$$\mathrm{ord}_\infty(f) \; + \; \frac{1}{2}\mathrm{ord}_{\mathrm{i}}(f) \; + \; \frac{1}{3}\mathrm{ord}_\rho(f) \; + \; \sum_{z \in \mathcal{F}^\circ} \mathrm{ord}_z(f) \; = \; \frac{k}{12}, \tag{82}$$

where $\mathcal{F}^\circ$ is the interior of a fundamental domain for $\mathrm{PSL}_2(\mathbb{Z})$ and $\mathrm{ord}_z(f) \geq 0$ is the vanishing order at z.

Corollary B.2 (finite determination from initial q-coefficients)**.** *Let f, g be holomorphic modular forms of weight k on $\mathrm{SL}_2(\mathbb{Z})$ with q-expansions*

$$f(\tau) = \sum_{n \geq 0} a_n q^n, \qquad g(\tau) = \sum_{n \geq 0} b_n q^n, \qquad q = \mathrm{e}^{2\pi \mathrm{i} \tau}.$$

If $a_n = b_n$ for all $0 \leq n \leq M$ with $M > \frac{k}{12}$, then $f = g$. Equivalently, a weight-k form is uniquely determined by its first $\lfloor k/12 \rfloor + 1$ coefficients.

Proof. The difference $h = f - g$ is a holomorphic modular form of weight k. If $a_n = b_n$ for $0 \leq n \leq M$, then $h(\tau) = O(q^{M+1})$ at ∞, i.e. $\mathrm{ord}_\infty(h) \geq M + 1$. If $h \neq 0$, Theorem B.1 implies $\mathrm{ord}_\infty(h) \leq k/12$, a contradiction when $M > k/12$. Hence $h = 0$ and $f = g$. □

B.3 Star discrepancy and the Koksma inequality

For a point set $P_N = \{x_0, \dots, x_{N-1}\} \subset [0,1)$, the one-dimensional star discrepancy is

$$D_N^*(P_N) = \sup_{0 \le u \le 1} \left| \frac{1}{N} \sum_{t=0}^{N-1} \mathbf{1}_{[0,u)}(x_t) - u \right|. \tag{83}$$

Definition B.3 (variation for complex-valued functions)**.** *For a complex-valued function $f : [0,1] \to \mathbb{C}$, define its (Jordan) variation by*

$$\mathrm{Var}(f) := \mathrm{Var}(\Re f) + \mathrm{Var}(\Im f), \tag{84}$$

where $\mathrm{Var}(\Re f)$ and $\mathrm{Var}(\Im f)$ are the usual real-valued Jordan variations.

Theorem B.4 (Koksma inequality, 1D)**.** *If $f : [0,1] \to \mathbb{C}$ has bounded variation (Jordan variation) $\mathrm{Var}(f) < \infty$, then*

$$\left| \frac{1}{N} \sum_{t=0}^{N-1} f(x_t) - \int_0^1 f(x)\,\mathrm{d}x \right| \le \mathrm{Var}(f)\, D_N^*(P_N). \tag{85}$$

Remark B.5. *See [19,27] for classical statements and proofs. With Definition B.3, the complex-valued inequality follows immediately by applying the real-valued Koksma inequality to $\Re f$ and $\Im f$ and using the triangle inequality:*

$$|\Delta(f)| \le |\Delta(\Re f)| + |\Delta(\Im f)| \le \big(\mathrm{Var}(\Re f) + \mathrm{Var}(\Im f)\big) D_N^*(P_N) = \mathrm{Var}(f)\, D_N^*(P_N), \tag{86}$$

where $\Delta(g) = \frac{1}{N}\sum g(x_t) - \int_0^1 g$.

B.4 Denjoy–Koksma at convergent lengths

Let $\alpha = [0; a_1, a_2, \dots]$ be irrational with convergents p_n/q_n. For the irrational rotation $R_\alpha(x) = x + \alpha \pmod 1$, the Denjoy–Koksma inequality controls Birkhoff sums at convergent lengths [16, 17, 27].

Theorem B.6 (Denjoy–Koksma inequality (rotation))**.** *If $f : [0,1] \to \mathbb{R}$ has bounded variation and $\int_0^1 f(x)\,\mathrm{d}x = 0$, then for every n and all x,*

$$\left| \sum_{t=0}^{q_n - 1} f(x + t\alpha) \right| \le \mathrm{Var}(f). \tag{87}$$

B.5 Ostrowski block decomposition and the digit bound

Write N in its Ostrowski expansion $N = \sum_{j=0}^{m} b_j q_j$ associated with α. Then the orbit segment $\{x + t\alpha\}_{t=0}^{N-1}$ can be partitioned into blocks of consecutive lengths q_j repeated b_j times, up to shifts of the starting point. Applying Theorem B.6 to each block yields a standard digit bound for Birkhoff sums:

$$\left| \sum_{t=0}^{N-1} f(x + t\alpha) - N \int_0^1 f \right| \le \mathrm{Var}(f) \sum_{j=0}^{m} b_j. \tag{88}$$

Applying this to interval indicator functions and combining with Theorem B.4 yields the discrepancy bound used in Corollary 5.8. Concretely, for $f_u(x) = \mathbf{1}_{[0,u)}(x) - u$ we have $\int_0^1 f_u = 0$ and $\mathrm{Var}(f_u) \le 2$, hence

$$\left| \frac{1}{N} \sum_{t=0}^{N-1} \mathbf{1}_{[0,u)}(x + t\alpha) - u \right| \le \frac{2}{N} \sum_{j=0}^{m} b_j, \tag{89}$$

and taking the supremum over $u \in [0,1]$ gives (38).

A constant-type corollary (explicit $(\log N)/N$ rate). If $\alpha = [0; a_1, a_2, \dots]$ has bounded partial quotients $a_n \le A$, then Ostrowski digits satisfy $b_j \le a_{j+1} \le A$, hence $\sum_{j=0}^{m} b_j \le A(m+1)$. Moreover, the convergent denominators satisfy $q_{n+1} = a_{n+1}q_n + q_{n-1} \ge q_n + q_{n-1}$, so $q_n \ge F_n$ for Fibonacci numbers F_n. If $q_m \le N < q_{m+1}$, then $F_m \le N$, hence $m \le 2 + \log_\varphi N$. Combining these estimates with (38) yields

$$D_N^*(P_N) \le \frac{2A(2 + \log_\varphi N)}{N}, \tag{90}$$

recovering the standard $O((\log N)/N)$ discrepancy rate for constant-type rotations (cf. [19]).

B.6 Exact star discrepancy at convergent lengths (closed form)

Proposition B.7 (Convergent-length star discrepancy for a Kronecker orbit)**.** *Let $\alpha \in (0,1)\setminus\mathbb{Q}$ and let p/q be a reduced rational satisfying*

$$0 < \left|\alpha - \frac{p}{q}\right| < \frac{1}{q^2}. \tag{91}$$

Consider the Kronecker point set

$$P_q(\alpha) := \{\{t\alpha\} : t = 0, 1, \dots, q-1\} \subset [0,1). \tag{92}$$

Then the one-dimensional star discrepancy satisfies

$$D_q^*(P_q(\alpha)) = \begin{cases} \dfrac{1}{q}, & \dfrac{p}{q} < \alpha, \\[2mm] \dfrac{1}{q} + (q-1)\left(\dfrac{p}{q} - \alpha\right), & \dfrac{p}{q} > \alpha. \end{cases} \tag{93}$$

Proof. Write $\delta := \alpha - \frac{p}{q}$ and note that for $0 \le t \le q-1$ one has $|t\delta| < (q-1)/q^2 < 1/q$. Let $r_t \in \{0, 1, \dots, q-1\}$ be the residue $r_t \equiv tp \pmod q$; since $\gcd(p,q) = 1$, the map $t \mapsto r_t$ is a permutation.

Case 1: $\delta > 0$ (i.e. $p/q < \alpha$). For each t,

$$\{t\alpha\} = \left\{\frac{tp}{q} + t\delta\right\} = \frac{r_t}{q} + t\delta \in \left[\frac{r_t}{q}, \frac{r_t + 1}{q}\right), \tag{94}$$

where the last inclusion uses $0 \le t\delta < 1/q$ and $r_t = q-1$ is interpreted modulo 1. Hence each interval $[j/q, (j+1)/q)$ contains exactly one point of $P_q(\alpha)$, which implies $D_q^*(P_q(\alpha)) \le 1/q$. Since $0 \in P_q(\alpha)$, one also has $D_q^*(P_q(\alpha)) \ge 1/q$ (take $u \downarrow 0$), so equality holds.

Case 2: $\delta < 0$ (i.e. $p/q > \alpha$). Let $\delta' := -\delta = \frac{p}{q} - \alpha > 0$. For $t \ge 1$, $r_t \ne 0$ so $r_t/q \ge 1/q$, and

$$\{t\alpha\} = \left\{\frac{tp}{q} - t\delta'\right\} = \frac{r_t}{q} - t\delta' \in \left(\frac{r_t - 1}{q}, \frac{r_t}{q}\right), \tag{95}$$

since $0 < t\delta' < 1/q$. Thus every interval $[j/q, (j+1)/q)$ with $j = 0, \dots, q-2$ contains exactly one point coming from the unique $t \in \{1, \dots, q-1\}$ with $r_t = j+1$, while the point $0 \in P_q(\alpha)$ lies in $[0, 1/q)$. The maximal discrepancy occurs at the right endpoints and equals $\frac{1}{q} + (q-1)\delta'$. □

B.7 Golden branch: Fibonacci convergents and the $1 + 1/\sqrt{5}$ constant

Let $\varphi = (1+\sqrt{5})/2$ and $\alpha = \varphi^{-1}$. The convergents of α are Fibonacci ratios $\frac{p_n}{q_n} = \frac{F_{n-1}}{F_n}$. Proposition B.7 implies that for odd n (when $p_n/q_n < \alpha$) one has $D^*_{F_n} = 1/F_n$, while for even n (when $p_n/q_n > \alpha$) one has

$$D^*_{F_n} = \frac{1}{F_n} + (F_n - 1)\left(\frac{F_{n-1}}{F_n} - \alpha\right). \tag{96}$$

Using Binet's formula and the asymptotic $F_n \sim \varphi^n/\sqrt{5}$, one obtains

$$F_n^2 \left(\frac{F_{n-1}}{F_n} - \alpha\right) \to \frac{1}{\sqrt{5}} \qquad (n \to \infty,\ n \text{ even}), \tag{97}$$

and therefore

$$F_n\, D^*_{F_n} \to 1 + \frac{1}{\sqrt{5}} \qquad (n \to \infty,\ n \text{ even}), \tag{98}$$

which is the constant observed in discrepancy scaling on the golden branch.

B.8 A crude variation bound for the sliced integrand

In Theorem 5.5, the bounded-variation assumption is imposed on

$$g_{n,y}(x) = F_y(x)\, \mathrm{e}^{-2\pi \mathrm{i} n x} = f(x + \mathrm{i}y)\, \mathrm{e}^{-2\pi \mathrm{i} n x}. \tag{99}$$

In concrete modular-form settings, F_y is smooth in x for every fixed $y > 0$ and admits termwise differentiation under absolute convergence of (30). A crude bound is obtained from total variation via an L^1 derivative estimate when $g_{n,y}$ is absolutely continuous:

$$\mathrm{Var}(g_{n,y}) \le \int_0^1 |g'_{n,y}(x)|\, \mathrm{d}x \le \int_0^1 |F'_y(x)|\, \mathrm{d}x + 2\pi n \int_0^1 |F_y(x)|\, \mathrm{d}x. \tag{100}$$

For specific choices of f (e.g. E_4, E_6, Δ, j), the L^1 norms above can be bounded using coefficient growth and geometric tail bounds in $|q| = \mathrm{e}^{-2\pi y}$.

B.9 Uniform convergence on slices and sufficient conditions for coefficient recovery

The slice–projection identity of Theorem 5.2 is stated under an absolute-uniform convergence assumption at fixed $y > 0$. For the modular objects used in this manuscript, that assumption follows from standard coefficient-growth bounds.

Proposition B.8 (polynomial growth implies uniform slice convergence)**.** *Let $(a_n)_{n\ge 0}$ satisfy a polynomial growth bound $|a_n| \le C(1+n)^A$ for some constants $C, A > 0$, and define*

$$f(\tau) = \sum_{n \ge 0} a_n \mathrm{e}^{2\pi \mathrm{i} n \tau}, \qquad \tau = x + \mathrm{i}y. \tag{101}$$

Then for every $y_0 > 0$ the series for f converges absolutely and uniformly on $\{(x,y) : x \in [0,1],\ y \ge y_0\}$. In particular, for each fixed $y > 0$, the slice $F_y(x) = f(x + \mathrm{i}y)$ admits termwise integration on $[0,1]$ and Theorem 5.2 applies.

Proof. For $y \ge y_0$ one has $|\mathrm{e}^{2\pi \mathrm{i} n \tau}| = \mathrm{e}^{-2\pi n y} \le \mathrm{e}^{-2\pi n y_0}$. Thus

$$|a_n \mathrm{e}^{2\pi \mathrm{i} n \tau}| \le C(1+n)^A \mathrm{e}^{-2\pi n y_0}. \tag{102}$$

Since $\sum_{n\ge 0} (1+n)^A \mathrm{e}^{-2\pi n y_0} < \infty$, the Weierstrass M-test gives absolute uniform convergence on the stated domain. Termwise integration on $[0,1]$ follows from uniform absolute convergence at fixed $y > 0$. □

Remark B.9 (bounded variation via Fourier coefficient sums)**.** *Under the same polynomial bound, the derivative series with respect to x also converges absolutely and uniformly for $y \geq y_0$ because an extra factor n preserves summability against $\mathrm{e}^{-2\pi n y_0}$. Hence F_y is C^1 in x, and $g_{n,y}(x) = F_y(x)\mathrm{e}^{-2\pi \mathrm{i} n x}$ is absolutely continuous. Moreover, if $g_{n,y}(x) = \sum_{m\in\mathbb{Z}} c_m \mathrm{e}^{2\pi \mathrm{i} m x}$ is its Fourier series, then*

$$\mathrm{Var}(g_{n,y}) = \int_0^1 |g'_{n,y}(x)|\,\mathrm{d}x \leq 2\pi \sum_{m\in\mathbb{Z}} |m|\,|c_m|. \tag{103}$$

For q-expansions with nonnegative indices, one has $c_{k-n} = a_k \mathrm{e}^{-2\pi k y}$, so $\mathrm{Var}(g_{n,y})$ can be bounded explicitly in terms of coefficient-growth majorants, as in Appendix B.11.

Remark B.10 (modular-form coefficient growth (standard input))**.** *For holomorphic modular forms of level 1, Fourier coefficients have polynomial growth. For Eisenstein series, one has $a_n = O(n^{k-1})$ (e.g. [22,25]). For cusp forms, Deligne's theorem (Ramanujan–Petersson) implies $a_n = O_\varepsilon(n^{(k-1)/2+\varepsilon})$ (e.g. [26, 33]). Thus Proposition B.8 applies to the modular-form objects used in the slice–sampling examples.*

B.10 Deligne/Hecke bounds for Ramanujan's $\tau(n)$ (explicit majorants)

Let $\Delta(\tau) = \sum_{n\geq 1} \tau(n) q^n$ denote the normalized weight-12 Hecke eigen cusp form on $\mathrm{SL}_2(\mathbb{Z})$.

Proposition B.11 (Ramanujan–Petersson/Deligne bound (standard))**.** *For every prime p one has*

$$|\tau(p)| \leq 2p^{11/2}. \tag{104}$$

Remark B.12. *This is a special case of Deligne's proof of the Weil conjectures. See [33, 35] for the Ramanujan–Petersson bounds for Hecke eigenvalues of modular forms.*

Proposition B.13 (global coefficient bound via Hecke multiplicativity)**.** *For every $n \geq 1$,*

$$|\tau(n)| \leq d(n)\, n^{11/2}, \tag{105}$$

where $d(n)$ is the divisor-counting function. In particular, using the trivial estimate $d(n) \leq 2\sqrt{n}$ one obtains the explicit crude majorant

$$|\tau(n)| \leq 2n^6, \qquad n \geq 1. \tag{106}$$

Proof. For prime powers one has the Hecke recursion

$$\tau(p^{r+1}) = \tau(p)\tau(p^r) - p^{11}\tau(p^{r-1}), \qquad r \geq 1, \tag{107}$$

so the local Euler factor is $1 - \tau(p)p^{-s} + p^{11}p^{-2s}$ and the standard bound $|\tau(p^r)| \leq (r+1)p^{11r/2}$ follows from Proposition B.11 (see, e.g., [22, 26]). Multiplicativity on coprime integers then yields $|\tau(n)| \leq d(n)n^{11/2}$ for general n. Finally, $d(n) \leq 2\sqrt{n}$ is immediate from pairing divisors $d \leftrightarrow n/d$. □

B.11 An explicit $\mathrm{Var}(g_{n,y})$ bound for E_4

For the weight-4 Eisenstein series

$$E_4(\tau) = 1 + 240 \sum_{k\geq 1} \sigma_3(k)\, q^k, \qquad q = \mathrm{e}^{2\pi \mathrm{i}\tau}, \tag{108}$$

define, as in Section 5,

$$g_{n,y}(x) = E_4(x + \mathrm{i}y)\, \mathrm{e}^{-2\pi \mathrm{i} n x}. \tag{109}$$

Fix $y > 0$ and write $r = \mathrm{e}^{-2\pi y} = |q| \in (0,1)$. Then $g_{n,y}$ has an absolutely convergent Fourier expansion

$$g_{n,y}(x) = \sum_{m\in\mathbb{Z}} c_m \, \mathrm{e}^{2\pi \mathrm{i} m x}, \qquad c_{k-n} = \begin{cases} r^0, & k = 0, \\ 240\,\sigma_3(k)\, r^k, & k \geq 1, \end{cases} \tag{110}$$

and is absolutely continuous. Hence $\mathrm{Var}(g_{n,y}) = \int_0^1 |g'_{n,y}(x)|\,\mathrm{d}x$. Moreover,

$$g'_{n,y}(x) = 2\pi\mathrm{i} \sum_{m\in\mathbb{Z}} m c_m \, \mathrm{e}^{2\pi \mathrm{i} m x}, \qquad |g'_{n,y}(x)| \leq 2\pi \sum_{m\in\mathbb{Z}} |m|\,|c_m|, \tag{111}$$

so

$$\mathrm{Var}(g_{n,y}) \leq 2\pi \sum_{m\in\mathbb{Z}} |m|\,|c_m| = 2\pi \left(n + 240 \sum_{k\geq 1} |k-n| \sigma_3(k)\, r^k \right). \tag{112}$$

Using the classical bound $\sigma_3(k) \leq \zeta(3)\, k^3$ (e.g. [25]), we obtain the explicit estimate

$$\mathrm{Var}(g_{n,y}) \leq 2\pi \left(n + 240\,\zeta(3) \sum_{k\geq 1} (k+n)\, k^3\, r^k \right) = 2\pi \left(n + 240\,\zeta(3) \big(S_4(r) + n S_3(r) \big) \right), \tag{113}$$

where

$$S_3(r) = \sum_{k\geq 1} k^3 r^k = \frac{r(1+4r+r^2)}{(1-r)^4}, \qquad S_4(r) = \sum_{k\geq 1} k^4 r^k = \frac{r(1+11r+11r^2+r^3)}{(1-r)^5}. \tag{114}$$

Combining (113) with Theorem 5.5 yields a fully explicit coefficient-recovery bound for E_4.

B.12 An explicit $\mathrm{Var}(g_{n,y})$ bound for E_6

For the weight-6 Eisenstein series

$$E_6(\tau) = 1 - 504 \sum_{k\geq 1} \sigma_5(k)\, q^k, \qquad q = \mathrm{e}^{2\pi \mathrm{i} \tau}, \tag{115}$$

define

$$g_{n,y}(x) = E_6(x + \mathrm{i}y)\, \mathrm{e}^{-2\pi \mathrm{i} n x}. \tag{116}$$

Fix $y > 0$ and write $r = \mathrm{e}^{-2\pi y} = |q| \in (0,1)$. As in the E_4 case, $g_{n,y}$ is absolutely continuous and

$$\mathrm{Var}(g_{n,y}) \leq 2\pi \left(n + 504 \sum_{k\geq 1} |k-n|\, \sigma_5(k)\, r^k \right). \tag{117}$$

Using $\sigma_5(k) \leq \zeta(5)\, k^5$ (e.g. [25]) and $|k-n| \leq k+n$, we obtain

$$\mathrm{Var}(g_{n,y}) \leq 2\pi \left(n + 504\,\zeta(5) \sum_{k\geq 1} (k+n)\, k^5\, r^k \right) = 2\pi \left(n + 504\,\zeta(5) \big(S_6(r) + n S_5(r) \big) \right), \tag{118}$$

where

$$S_5(r) = \sum_{k\geq 1} k^5 r^k = \frac{r(1+26r+66r^2+26r^3+r^4)}{(1-r)^6}, \tag{119}$$

$$S_6(r) = \sum_{k\geq 1} k^6 r^k = \frac{r(1+57r+302r^2+302r^3+57r^4+r^5)}{(1-r)^7}. \tag{120}$$

Combining (118) with Theorem 5.5 yields a fully explicit coefficient-recovery bound for E_6.

B.13 Tail bounds for Eisenstein q-series (explicit constants)

For level 1, the Eisenstein series admit the classical q-expansions (e.g. [22, 25])

$$E_4(\tau) = 1 + 240 \sum_{n\geq 1} \sigma_3(n)\, q^n, \qquad E_6(\tau) = 1 - 504 \sum_{n\geq 1} \sigma_5(n)\, q^n, \qquad q = \mathrm{e}^{2\pi \mathrm{i}\tau}. \tag{121}$$

Fix $|q| = r \in (0,1)$ and define the truncations $E_4^{(N)} = 1 + 240 \sum_{n=1}^{N} \sigma_3(n) q^n$ and $E_6^{(N)} = 1 - 504 \sum_{n=1}^{N} \sigma_5(n) q^n$. Using the divisor-sum bound $\sigma_k(n) \leq \zeta(k)\, n^k$ (e.g. [25]), we obtain explicit tail bounds.

Proposition B.14 (explicit tails for E_4 and E_6)**.** *Let $r \in (0,1)$ and $N \geq 1$. Then*

$$|E_4(\tau) - E_4^{(N)}(\tau)| \leq 240\, \zeta(3) \sum_{n=N+1}^{\infty} n^3 r^n \tag{122}$$

$$\leq 240\, \zeta(3)\, r^{N+1} \left(\frac{(N+1)^3}{1-r} + \frac{3(N+1)^2 r}{(1-r)^2} \right. \tag{123}$$

$$\left. + \frac{3(N+1) r(1+r)}{(1-r)^3} + \frac{r(1+4r+r^2)}{(1-r)^4} \right),$$

and

$$\begin{aligned} |E_6(\tau) - E_6^{(N)}(\tau)| \leq 504\, \zeta(5) \sum_{n=N+1}^{\infty} n^5 r^n \;\leq\; 504\, \zeta(5)\, r^{N+1} \Bigg(& \frac{(N+1)^5}{1-r} \\ & + \frac{5(N+1)^4 r}{(1-r)^2} \\ & + \frac{10(N+1)^3 r(1+r)}{(1-r)^3} \\ & + \frac{10(N+1)^2 r(1+4r+r^2)}{(1-r)^4} \\ & + \frac{5(N+1) r(1+11r+11r^2+r^3)}{(1-r)^5} \\ & + \frac{r(1+26r+66r^2+26r^3+r^4)}{(1-r)^6} \Bigg), \end{aligned} \tag{124}$$

Remark B.15. *The bounds* (122) *and* (124) *are obtained by expanding $(N+1+m)^p$ and using the standard generating functions for $\sum_{m\geq 0} m^j r^m$. In particular,*

$$\sum_{m\geq 0} m^4 r^m = \frac{r(1+11r+11r^2+r^3)}{(1-r)^5}, \tag{125}$$

$$\sum_{m\geq 0} m^5 r^m = \frac{r(1+26r+66r^2+26r^3+r^4)}{(1-r)^6}, \tag{126}$$

which appear explicitly in the E_6 tail bound.

B.14 Abel-first regularization and alternative summability prescriptions (standard facts)

Assumption R1 stipulates a canonical convention for extracting a finite part from regulated orbit traces and related divergent sums: "Abel first, then limit". This subsection records standard summability facts that justify Abel as a conservative choice and clarify the relation to other classical prescriptions.

Abel summability for sequences. Given a sequence $(s_t)_{t\geq 0}$, define its Abel mean by the regulated averages

$$A(r) := (1-r)\sum_{t=0}^{\infty} s_t\, r^t, \qquad 0 < r < 1. \tag{127}$$

If $\lim_{r\to 1^-} A(r)$ exists, we say (s_t) is Abel summable and call the limit its Abel sum. This damping has a direct operational interpretation as an exponential "forgetting" or finite-coherence-time filter.

Cesàro and Abel. Classical Tauberian theory relates Abel and Cesàro summability. In particular, Cesàro summability implies Abel summability with the same sum (and under additional mild hypotheses one has converses); see [11] for standard statements and proofs. Thus adopting Abel regularization is a canonical way to select a finite part that is consistent with (at least) Cesàro when the latter applies.

Borel-type regularizations. Borel summability is another classical prescription that can assign finite values to divergent series by analytic continuation of an exponential transform; see [11]. The present manuscript does not require Borel summation as an input: the main quantitative recovery statements are finite-N bounds and therefore do not depend on any infinite-time regularization. When divergent orbit traces arise in extensions of the framework, Abel-first provides a minimal and physically interpretable convention compatible with the intrinsic damping already present in the cusp modulus $|q| = \mathrm{e}^{-2\pi y}$ (Section 5.7) and with the general layer discipline (Appendix D.8).

B.15 Gauss measure mean of the roof function

Let μ denote the Gauss invariant measure for the Gauss map,

$$\mathrm{d}\mu(\xi) = \frac{1}{\log 2}\frac{\mathrm{d}\xi}{1+\xi}, \qquad \xi \in (0,1). \tag{128}$$

The roof function in Theorem 4.1 is $r(\xi) = -2\log\xi$.

Proposition B.16 (closed-form mean)**.** *One has*

$$\int_0^1 (-\log\xi)\,\mathrm{d}\mu(\xi) = \frac{\pi^2}{12\log 2}, \qquad \int_0^1 r(\xi)\,\mathrm{d}\mu(\xi) = \frac{\pi^2}{6\log 2}. \tag{129}$$

Proof. Expand $(1+\xi)^{-1} = \sum_{n=0}^{\infty}(-1)^n\xi^n$ for $\xi \in (0,1)$ and integrate termwise:

$$\int_0^1 \frac{-\log\xi}{1+\xi}\,\mathrm{d}\xi = \sum_{n=0}^{\infty}(-1)^n\int_0^1 \xi^n(-\log\xi)\,\mathrm{d}\xi = \sum_{n=0}^{\infty}(-1)^n\frac{1}{(n+1)^2} \tag{130}$$

$$= \sum_{m=1}^{\infty}\frac{(-1)^{m-1}}{m^2} = (1-2^{1-2})\zeta(2) = \frac{1}{2}\cdot\frac{\pi^2}{6} = \frac{\pi^2}{12}. \tag{131}$$

Dividing by $\log 2$ gives the first identity, and the second follows by multiplying by 2. □

B.16 Derivation of the Gauss digit law

Write the continued fraction of $\xi \in (0,1)$ as $\xi = [0; a_1, a_2, \dots]$ so that $a_1 = \lfloor 1/\xi \rfloor$.

Proposition B.17 (Gauss digit probabilities)**.** *For the Gauss invariant measure* $\mathrm{d}\mu(\xi) = \frac{1}{\log 2}\frac{\mathrm{d}\xi}{1+\xi}$ *one has, for every* $k \geq 1$*,*

$$\mu(a_1 = k) = \log_2\!\left(1 + \frac{1}{k(k+2)}\right). \tag{132}$$

Proof. The event $\{a_1 = k\}$ is equivalent to $\frac{1}{k+1} < \xi \le \frac{1}{k}$. Therefore

$$\mu(a_1 = k) = \frac{1}{\log 2} \int_{1/(k+1)}^{1/k} \frac{\mathrm{d}\xi}{1+\xi} = \frac{1}{\log 2} \left[\log(1+\xi)\right]_{1/(k+1)}^{1/k} \tag{133}$$

$$= \frac{1}{\log 2} \log\!\left(\frac{1+1/k}{1+1/(k+1)}\right) = \frac{1}{\log 2} \log\!\left(\frac{(k+1)^2}{k(k+2)}\right) = \log_2\!\left(1 + \frac{1}{k(k+2)}\right). \tag{134}$$

□

B.17 Gauss–Kuzmin convergence (standard exponential relaxation)

Theorem B.18 (Gauss–Kuzmin)**.** *Let $G : (0,1) \to (0,1)$ be the Gauss map and let μ be its invariant probability measure. For a broad class of absolutely continuous initial distributions ν on $(0,1)$ (e.g. densities of bounded variation), there exist constants $C > 0$ and $0 < \lambda < 1$ such that for all $n \ge 1$,*

$$\sup_{x \in (0,1]} \left|\nu(G^{-n}((0,x])) - \mu((0,x])\right| \le C\,\lambda^n. \tag{135}$$

Remark B.19. *This is the classical Gauss–Kuzmin theorem (and its refinements via transfer-operator spectral gaps). We treat it as a standard input from metrical continued-fraction theory; see [23].*

C Sharpened protocol statements: why $X(1)$, worked recovery, and falsifiable closure

C.1 Why the modular curve $X(1)$ as mother space? Minimality under protocol requirements

Section 2.3 fixes a mother space and a canonical climb (geodesic/Gauss suspension) to make the "scale axis" computable and audit-friendly. The choice $X(1) = \mathrm{PSL}_2(\mathbb{Z})\backslash(\mathbb{H} \cup \{\text{cusps}\})$ is not meant as a claim that other arithmetic surfaces are impossible; rather, it is the minimal choice once one imposes a small set of protocol-driven requirements.

Protocol requirements. The closed chain in this paper relies on three structural inputs:

- **A cusp with a canonical continuous–discrete coordinate.** To extract an integer spectrum by Fourier projection with an explicit damping modulus, we require a non-compact end admitting a canonical local parameter $q = \mathrm{e}^{2\pi \mathrm{i} \tau}$ (Section 5.1). Compact arithmetic quotients (e.g. Shimura curves) may carry Hecke correspondences but have no cusp, hence no q-expansion interface.
- **A canonical cross-scale flow with digit syntax.** We require an intrinsic flow whose Poincaré return coding produces continued-fraction digits and an additive "scale time" (Theorem 4.1 and Section 4.2), so that the same parameter α controlling scan readout also controls a computable digit law under the climb.
- **A prime-indexed commuting correspondence algebra.** To close the discrete layer by an auditable prime skeleton, we require a large commensurator giving rise to Hecke operators/correspondences and their prime-generated algebraic closure (Section 6).

A minimality statement within congruence covers. Among modular curves arising from congruence subgroups of $\mathrm{PSL}_2(\mathbb{Z})$, the above requirements single out level 1 as the unique one-cusp option.

Proposition C.1 (one-cusp congruence minimality (standard))**.** *Let $\Gamma \leq \mathrm{PSL}_2(\mathbb{Z})$ be a congruence subgroup of finite index. If the modular curve $X(\Gamma)$ has a single cusp class, then $\Gamma = \mathrm{PSL}_2(\mathbb{Z})$ and hence $X(\Gamma) = X(1)$.*

Remark C.2. *For standard cusp-count formulas for congruence subgroups (e.g. $\Gamma_0(N)$, $\Gamma_1(N)$, $\Gamma(N)$) and the fact that proper congruence subgroups have at least two cusps, see [22, 25].*

A no-go for non-arithmetic quotients (conceptual). Non-arithmetic finite-area hyperbolic quotients do not carry a nontrivial commuting Hecke algebra: the commensurator is discrete and does not generate prime-indexed correspondences. In the present framework, this blocks the "prime skeleton" closure step and forces the discrete spectrum to be controlled by different (non-Hecke) structures. This is consistent with the commensurator-based arithmeticity dichotomy in the theory of lattices [12].

In this sense, $X(1)$ is singled out as the simplest hyperbolic orbifold simultaneously exhibiting a cusp q-interface, a canonical digit-coded climb, and a prime-generated correspondence algebra. Congruence covers and higher-level modular curves remain compatible variants, but they introduce additional discrete data (more cusps/levels) beyond the minimal protocol footprint.

A minimal covolume uniqueness theorem (one cusp). If one further asks for the simplest possible hyperbolic mother space under the *single-cusp* constraint, then $X(1)$ is also uniquely minimal in hyperbolic area.

Proposition C.3 (minimal area among one-cusp hyperbolic orbifolds (standard))**.** *Let Y be an orientable finite-area hyperbolic 2-orbifold with exactly one cusp. Then*

$$\mathrm{Area}(Y) \geq \frac{\pi}{3}. \tag{136}$$

Moreover, equality holds if and only if Y has orbifold signature $(g; m_1, m_2; s) = (0; 2, 3; 1)$, in which case Y is (isometric to) the modular orbifold $X(1) = \mathrm{PSL}_2(\mathbb{Z})\backslash\mathbb{H}$.

Proof. Let Y have signature $(g; m_1, \ldots, m_r; s)$ with genus $g \geq 0$, elliptic orders $m_j \geq 2$, and $s = 1$ cusp. Orbifold Gauss–Bonnet gives

$$\mathrm{Area}(Y) = 2\pi\left(2g - 2 + s + \sum_{j=1}^{r}\left(1 - \frac{1}{m_j}\right)\right) = 2\pi\left(2g - 1 + \sum_{j=1}^{r}\left(1 - \frac{1}{m_j}\right)\right), \tag{137}$$

see, e.g., [38].

If $g \geq 1$, then $2g - 1 \geq 1$ and the sum is nonnegative, so $\mathrm{Area}(Y) \geq 2\pi > \pi/3$. Thus the minimum occurs at $g = 0$, where positivity of area forces

$$-1 + \sum_{j=1}^{r}\left(1 - \frac{1}{m_j}\right) > 0 \quad \Longleftrightarrow \quad \sum_{j=1}^{r}\frac{1}{m_j} < r - 1.$$

If $r \geq 3$, then $\sum_{j=1}^{r}\frac{1}{m_j} \leq r/2$, hence

$$\mathrm{Area}(Y) = 2\pi\left(r - 1 - \sum_{j=1}^{r}\frac{1}{m_j}\right) \geq 2\pi\left(r - 1 - \frac{r}{2}\right) = \pi(r-2) \geq \pi > \pi/3.$$

So the minimum occurs at $r = 2$, in which case

$$\mathrm{Area}(Y) = 2\pi\Big(1 - \frac{1}{m_1} - \frac{1}{m_2}\Big), \qquad \frac{1}{m_1} + \frac{1}{m_2} < 1.$$

To minimize area, we maximize $\frac{1}{m_1} + \frac{1}{m_2}$ subject to $m_1, m_2 \geq 2$ and the strict inequality < 1. The maximal such sum is $\frac{1}{2} + \frac{1}{3} = \frac{5}{6}$, achieved by $(m_1, m_2) = (2, 3)$, yielding $\mathrm{Area}(Y) = 2\pi(1 - 5/6) = \pi/3$. This is exactly the signature of the modular orbifold $X(1)$, and the equality characterization follows. □

C.2 A fully worked model at finite resolution (explicit error budgets)

We now give a concrete model realizing the scan algebra and a finite-alphabet instrument, together with a fully explicit coefficient-recovery guarantee for a standard modular observable.

C.2.1 Effective Hilbert space, scan/readout unitaries, and a finite-alphabet instrument

Let $\mathcal{H}_{\mathrm{eff}} = L^2(\mathbb{R}/\mathbb{Z})$ and define the Weyl pair as in Axiom O6:

$$(U_{\mathrm{scan}}\psi)(x) = \psi(x + \alpha), \qquad (V\psi)(x) = \mathrm{e}^{2\pi \mathrm{i} x}\psi(x), \qquad \alpha \in (0,1) \setminus \mathbb{Q}.$$

Fix a resolution parameter $\varepsilon \in (0, 1)$ and let $K = \lceil 1/\varepsilon \rceil$. Define a partition of unity by interval windows $w_k^{(\varepsilon)} = \mathbf{1}_{I_k}$ with

$$I_k = [k/K, (k+1)/K), \qquad k = 0, 1, \ldots, K-1,$$

and define effects by spectral calculus of V:

$$E_k^{(\varepsilon)} = \int_{\mathbb{R}/\mathbb{Z}} w_k^{(\varepsilon)}(x)\, \mathrm{d}\Pi_V(x), \qquad \sum_{k=0}^{K-1} E_k^{(\varepsilon)} = \mathbf{1}.$$

At tick t, the scan orbit induces a phase point $x_t = x_0 + t\alpha \pmod 1$ (Section 3.2); the finite-alphabet readout returns the bin index k_t such that $x_t \in I_{k_t}$. Let $\widetilde{x}_t$ denote the bin midpoint:

$$\widetilde{x}_t = \frac{k_t + 1/2}{K}.$$

Then $|x_t - \widetilde{x}_t| \leq \varepsilon/2$.

C.2.2 A certified coefficient estimator with quantization and sampling terms

Fix $y > 0$ and a modular-form observable f with a convergent q-expansion at height y (Section 5.1). Define the slice $F_y(x) = f(x + \mathrm{i}y)$ and the integrand

$$g_{n,y}(x) = F_y(x)\, \mathrm{e}^{-2\pi \mathrm{i} n x}.$$

The ideal (continuum) coefficient identity is

$$a_n = \mathrm{e}^{2\pi n y} \int_0^1 g_{n,y}(x)\, \mathrm{d}x$$

(Theorem 5.2). At finite resolution and finite N, we use the quantized scan-sampled coefficient estimator of Definition 9.1 (Equation 77). Theorem 9.2 provides an explicit end-to-end bound including both discrepancy (sampling) and ε-quantization terms, while Remark 9.4 records how to add certified evaluation/truncation terms when f is computed via truncated q-series.

C.2.3 A worked modular observable: E_4 with explicit constants and exact-integer recovery

Take $f(\tau) = E_4(\tau) = 1 + 240\sum_{m\geq 1}\sigma_3(m)q^m$ (Appendix B.11). Then $a_0 = 1$ and $a_n = 240\,\sigma_3(n) \in \mathbb{Z}$ for $n \geq 1$. Appendix B.11 gives an explicit coefficient-sum bound

$$\|g'_{n,y}\|_\infty \leq 2\pi\left(n + 240\,\zeta(3)\big(S_4(r) + nS_3(r)\big)\right), \qquad r = \mathrm{e}^{-2\pi y},$$

and the same expression upper-bounds $\mathrm{Var}(g_{n,y})$. Combining with Theorem 9.2 yields a completely explicit bound in terms of (n, y, N, ε) and $D_N^*(P_N)$ (or its Ostrowski digit bounds, Appendix B.5). In arithmetic settings with $a_n \in \mathbb{Z}$, exact integer recovery follows from the rounding criterion in Corollary 9.5.

Corollary C.4 (parameter selection for E_4: explicit sufficient inequalities)**.** *Let $f = E_4$ and fix (n, y, N, ε) with $r = \mathrm{e}^{-2\pi y}$. Define the explicit constant*

$$B_{n,y}^{(4)} := 2\pi\left(n + 240\,\zeta(3)\big(S_4(r) + nS_3(r)\big)\right), \tag{138}$$

so that $\mathrm{Var}(g_{n,y}) \leq B_{n,y}^{(4)}$ and $\|g'_{n,y}\|_\infty \leq B_{n,y}^{(4)}$. Then

$$|\widehat{a}_{n,N}^{(\varepsilon)}(y) - a_n| \leq \mathrm{e}^{2\pi ny}\, B_{n,y}^{(4)}\left(D_N^*(P_N) + \frac{\varepsilon}{2}\right). \tag{139}$$

In particular:

- ***Convergent-length choice.*** *If p/q is a reduced rational with $0 < |\alpha - p/q| < 1/q^2$ and $N = q$, then Proposition B.7 implies $D_N^*(P_N) \leq 2/N$, hence*

$$|\widehat{a}_{n,N}^{(\varepsilon)}(y) - a_n| \leq \mathrm{e}^{2\pi ny}\, B_{n,y}^{(4)}\left(\frac{2}{N} + \frac{\varepsilon}{2}\right).$$

- ***Constant-type choice.*** *If $\alpha = [0; a_1, a_2, \ldots]$ has bounded partial quotients $a_j \leq A$, then Appendix B.5 gives $D_N^*(P_N) \leq \frac{2A(2+\log_\varphi N)}{N}$, hence*

$$|\widehat{a}_{n,N}^{(\varepsilon)}(y) - a_n| \leq \mathrm{e}^{2\pi ny}\, B_{n,y}^{(4)}\left(\frac{2A(2+\log_\varphi N)}{N} + \frac{\varepsilon}{2}\right).$$

In either case, the rounding criterion in Corollary 9.5 applies whenever the corresponding right-hand side is $< \frac{1}{2}$.

C.2.4 A certified numerical instance for E_4: exact recovery of $a_1 = 240$

To make the end-to-end bound concrete without any simulations, we record a single explicit parameter choice for which the rounding criterion is certified. Take the golden-branch scan slope $\alpha = \varphi^{-1} = [0; 1, 1, 1, \ldots]$ and choose a convergent-length sample size $N = 46368$ (a Fibonacci denominator of a convergent of α), so that Proposition B.7 implies $D_N^*(P_N) \leq 2/N$. Fix $n = 1$, $y = 0.7$, and a finite-alphabet resolution $\varepsilon = 10^{-4}$.

For $y = 0.7$ one has

$$r = \mathrm{e}^{-2\pi y} \approx 0.012299 < 0.0123, \qquad S_3(r) \approx 0.013561 < 0.0136, \qquad S_4(r) \approx 0.014876 < 0.0149,$$

and using the numerical bound $\zeta(3) < 1.202057$ in (138) (e.g. truncate $\zeta(3) = \sum_{m\geq 1} m^{-3}$ and bound the tail by $\sum_{m>K} m^{-3} < \int_K^\infty x^{-3}\mathrm{d}x = \frac{1}{2K^2}$ with $K = 20000$) one obtains

$$B_{1,0.7}^{(4)} < 57.83, \qquad \mathrm{e}^{2\pi\cdot 0.7} \approx 81.3068 < 81.31.$$

Using the convergent-length bound in Corollary C.4, we obtain the explicit numerical estimate

$$|\widehat{a}^{(\varepsilon)}_{1,N}(0.7) - a_1| \le \mathrm{e}^{2\pi\cdot 0.7}\, B^{(4)}_{1,0.7}\left(\frac{2}{46368} + \frac{10^{-4}}{2}\right) < 81.31 \cdot 57.83\left(\frac{2}{46368} + \frac{10^{-4}}{2}\right) < 0.44 < \frac{1}{2}.$$

Since $a_1 = 240\,\sigma_3(1) = 240 \in \mathbb{Z}$, Corollary 9.5 implies that rounding $\widehat{a}^{(\varepsilon)}_{1,N}(0.7)$ to the nearest integer recovers $a_1 = 240$ exactly.

C.3 Hecke operators at the protocol level: structural closure versus implementable channels

Section 6.2 already records the standard analytic action of T_p on modular forms as a finite average over explicit maps (double-coset correspondences) and its induced action on q-coefficients (Proposition 6.2). Two distinct protocol-level roles should be distinguished.

(i) Structural/audit role (used in this paper). In the closed Layer 0/1 chain, Hecke operators enter as *constraints on the recovered coefficient spectrum.* Once a candidate coefficient sequence (a_n) is obtained from the cusp slice by the estimator, the Hecke relations provide locally checkable closure constraints: coprime multiplicativity and the prime-power recursion (Section 6.6). These constraints are naturally interpreted as a prime-indexed "consistency check" on the discrete layer, and are directly falsifiable.

(ii) Implementable channel role (additional structure). If one insists on realizing T_p as a transformation on *observables* or *instruments* in $\mathcal{H}_{\mathrm{eff}}$, additional interface structure is required. At the level of modular observables, T_p mixes values at different heights (Equation (44)), so it is intrinsically cross-scale rather than a symmetry acting within a fixed slice. Operationally, implementing $O_f \mapsto O_{T_p f}$ would require an instrument family capable of accessing (or emulating) the branches $\tau \mapsto p\tau$ and $\tau \mapsto (\tau + b)/p$ across the relevant scale window, together with certified error control for the induced mixing. This is a natural extension problem but is not needed for the prime-skeleton closure used here.

C.4 Falsifiable predictions: prime-indexed regularities and distribution laws

When the recovered spectrum is hypothesized to arise from a normalized Hecke eigenform, the following prime-indexed statements become quantitative, falsifiable predictions about the discrete readout layer:

- **Exact algebraic closure.** For $(m, n) = 1$, one must have $a_{mn} = a_m a_n$, and for prime powers $a_{p^{r+1}} = a_p a_{p^r} - p^{k-1} a_{p^{r-1}}$ (Section 6.6).
- **Ramanujan–Petersson bounds.** For holomorphic cuspidal Hecke eigenforms, Deligne's theorem gives $|a_p| \le 2p^{(k-1)/2}$ (Appendix B.10 for Δ as a canonical example).
- **Sato–Tate statistics (when applicable).** For non-CM eigenforms, the normalized prime eigenvalues $a_p/(2p^{(k-1)/2})$ are expected to equidistribute with the Sato–Tate measure; see, e.g., [36, 39, 40].

In a protocol interpretation, failure of these prime-indexed regularities falsifies the claim that the observed discrete spectrum is governed by a Hecke eigenstructure.

C.5 QUE-type inputs and fluctuation bounds (optional strengthening)

The induced-measure picture in Section 3.3 is based on equidistribution of rotation orbits and discrepancy control. Independent from this, arithmetic quantum unique ergodicity (QUE) results provide equidistribution statements for Hecke eigenstates/eigenforms on arithmetic surfaces. For Maass Hecke eigenfunctions on $\mathrm{PSL}_2(\mathbb{Z})\backslash\mathbb{H}$, Lindenstrauss proved QUE for a full-density subsequence, with refinements by subsequent work [41]. For holomorphic Hecke eigenforms of large weight, mass equidistribution (a holomorphic QUE analogue) was established by Holowinsky and Soundararajan [42].

These results suggest an additional route to bounding readout fluctuations when the underlying observable sector is Hecke invariant: beyond generic discrepancy bounds, one can in principle use QUE-type estimates to control the variance of suitable test observables along arithmetic eigenbases. We do not use QUE as an input in the present paper; we record it as an optional strengthening direction aligned with the prime-skeleton semantics.

C.6 Vector-valued readouts and vector-valued Hecke operators (extension)

The scan–projection formalism extends to multiplets by replacing a scalar pointer with a finite family of commuting pointer phases (or, equivalently, a vector-valued instrument) and by allowing vector-valued modular/automorphic objects at the cusp interface. On the arithmetic side, this naturally leads to vector-valued modular forms and Hecke operators acting by matrices on the coefficient vectors. We record this as a straightforward extension path rather than a new premise.

C.7 QCA micro-models realizing O3/O6 (sketch)

At the constitution level, Axiom O3 posits a causally local discrete-time automorphism and Axiom O6 posits an effective Weyl pair. Locality-preserving unitary dynamics (quantum cellular automata / quantum walks) provide standard concrete realizations of O3 [43, 44]. In simple 1D models, shift/clock constructions generate Weyl-type relations on an effective boundary or observer sector, yielding a natural route to O6. Deriving the modular cusp interface and the appearance of a q-expansion-dominated readout from a specific QCA update rule remains an explicit model-building task; it is compatible with the present layer discipline but not required for the closed Layer 0/1 derivations in this paper.

D Limitations and open questions

The present paper isolates a closed Layer 0/1 chain and keeps Layer 2 narratives optional. Much of the mathematical content invoked along the chain—Gauss-map suspension coding of the modular geodesic flow, cusp q-expansions, Hecke relations, and discrepancy/variation bounds—is classical. The contribution is primarily a synthesis and protocol-level framing that exposes a concrete dependency chain and makes the finite-resolution extraction of discrete spectra auditable. The following limitations and open questions are explicit.

D.1 Scope and novelty

Most theorem-level inputs are standard results with well-established proofs (Appendix A). The contribution is a protocol-level synthesis that makes the cross-scale climb and the continuous–discrete interface quantitatively auditable at finite resources. Novelty claims are therefore best interpreted at the level of *interfaces* (scan orbit $\leftrightarrow$ slice sampling, slice $\leftrightarrow$ q-coefficients, coefficients $\leftrightarrow$ Hecke closure) and *closure mechanisms* (explicit end-to-end error budgets including finite-alphabet quantization, and exact integer recovery by rounding when $a_n \in \mathbb{Z}$; Theorem 9.2 and Corollary 9.5), rather than as new identities in classical modular theory.

D.2 Making protocol morphisms precise

Definition 7.1 treats "protocol equivalence" informally as preservation of Weyl structure and readout statistics, potentially implemented by Morita equivalence and state/instrument transport. A mathematically complete formulation requires:

- a precise choice of objects: allowed instruments and required continuity/regularity;
- a precise equivalence relation or morphism notion (what is preserved exactly, and with which error budgets);
- compatibility conditions with boundary/cusp interfaces.

D.3 Certified coefficient recovery under finite resources

The slice–sampling pipeline provides explicit discrepancy-based bounds (Theorem 5.5 and Corollary 5.8). Incorporating finite-alphabet readout yields an explicit sampling+quantization bound (Theorem 9.2) and, in arithmetic cases, an exact integer recovery criterion (Corollary 9.5). A fully certified numerical pipeline may additionally require:

- **Certified evaluation of $f(\tau)$ on slices.** When f is computed via truncated q-series, explicit tail bounds are required at fixed τ; for Eisenstein series these are given with constants in Appendix B.13, while for general cusp forms one needs explicit majorants compatible with the chosen computational representation (Remark 9.4).
- **Floating-point and instrument error propagation.** The bounds isolate sampling and quantization contributions, but a complete numerical budget must include floating-point rounding, conditioning, and any additional instrument noise as a function of (n, y, N, ε), especially in regimes where amplification by $\mathrm{e}^{2\pi ny}$ dominates.
- **Uniform regularity control.** The Koksma step is sharp only when $\mathrm{Var}(g_{n,y})$ and $\|g'_{n,y}\|_\infty$ are under control uniformly over the parameter ranges used in the protocol; see the next subsection.

D.4 Variation bounds, uniform constants, and stability windows

The coefficient-recovery bound

$$|\widehat{a}_{n,N}(y) - a_n| \le \mathrm{e}^{2\pi ny}\,\mathrm{Var}(g_{n,y})\,D_N^*(P_N)$$

is sensitive to the joint dependence of $\mathrm{Var}(g_{n,y})$ and the amplification factor $\mathrm{e}^{2\pi ny}$. Even when $D_N^*(P_N)$ is small, large variation or poor conditioning can destroy a meaningful guarantee.

For the most common modular objects, explicit bounds are available: Appendix B.8 records a general absolute-continuity estimate, and Appendix B.11–B.12 give closed-form y-dependent upper bounds for $\mathrm{Var}(g_{n,y})$ for E_4 and E_6 (in terms of $r = \mathrm{e}^{-2\pi y}$). Combined with the finite-alphabet bound (Theorem 9.2) and explicit tail bounds, these estimates already yield auditable end-to-end guarantees for standard Eisenstein observables (Appendix C.2 and Corollary C.4). For broader families, one still requires:

- explicit parameter ranges (n, y, N) for which the bound is numerically stable (a "scale window");
- explicit constants that remain uniform across the intended family of f (e.g. across a space of cusp forms or across a class of observables mapped to modular data);
- a principled way to trade off y (smoothing of slice data) against $\mathrm{e}^{2\pi ny}$ (amplification in coefficient recovery), beyond qualitative discussion.

D.5 Functorial uplift beyond GL_2

The paper only uses classical GL_2 modular objects in a minimal toy role. A genuine Langlands uplift requires:

- a target group G and a canonical replacement of the modular curve by a higher-dimensional arithmetic variety (e.g. Shimura data);
- a generalization of cusp discretization and prime-skeleton closure to G-Hecke data;
- functoriality constraints that identify which protocol equivalences correspond to which automorphic transfers.

D.6 Interfaces to externally specified observables

While Hecke spectra provide a rigid integer data layer, connecting it to any externally specified observable spectrum must be done with an explicit interface map and an error budget, without violating layer discipline. This remains a separate construction task.

D.7 Choosing the scan slope α and adapting N

Discrepancy control depends strongly on the Diophantine type of the rotation slope α. The Ostrowski digit bound (Corollary 5.8) makes this dependence auditable via the digit sum $\sum_j b_j$, but it also highlights a limitation: for α with large partial quotients (including Liouville-type parameters) the bound can deteriorate dramatically.

For constant-type rotations (bounded partial quotients), Appendix B.5 gives an explicit $O((\log N)/N)$ rate with constants depending on the bound on partial quotients. Moreover, at convergent lengths $N = q_m$ one has more refined and even closed-form discrepancy information (Appendix B.6). Pragmatically, this suggests two robust tactics for certified sampling:

- preferentially choose α of constant type (the golden branch is a canonical toy case);
- preferentially choose N near convergent denominators, while using the Ostrowski digit sum as an online diagnostic of "how expensive" a given N is in discrepancy terms.

D.8 R1 regularization: Abel-first conventions and their scope

Assumption R1 fixes a canonical prescription ("Abel first, then limit") for regulated-to-continuum passages along scan orbits when divergent sums or traces arise. In the present paper's main finite-N recovery pipeline, the core quantitative steps are finite-sample bounds (Koksma/Denjoy–Koksma and discrepancy) and do not require R1. The role of R1 is instead to specify a normalization convention in settings where one studies infinite-time orbit traces, distributional limits, or boundary limits in which a regulated parameter is sent to 1^- before taking a continuum limit (cf. the analogy between the cusp modulus $|q| = \mathrm{e}^{-2\pi y}$ and Abel damping in Section 5.7).

A sharper integration of R1 into a certified pipeline would require stating explicit conditions under which Abel regularization agrees with the analytic continuation or spectral regularization used on the modular side, and identifying whether it provides genuinely new control beyond the intrinsic damping already present in the cusp parameter y.

D.9 Empirical validation and practical tightness

The manuscript emphasizes certified bounds and explicit constants over empirical tightness. Numerical case studies could nonetheless complement the theory by testing:

- the practical tightness of discrepancy/digit bounds for realistic (α, N) choices;

- the dependence of $\mathrm{Var}(g_{n,y})$ on (n, y) for representative modular objects beyond E_4/E_6;
- the empirical stability window in (n, y, N) balancing smoothing against amplification.

Such experiments would clarify how conservative the explicit bounds are in typical regimes, but they are not required for the logical closure statements proved in this manuscript.

D.10 Related work: quasi-Monte Carlo, lattice rules, and transport-based metrics

Comparison with classical quadrature on the torus. The sampling scheme $x_t = x_0 + t\alpha \pmod 1$ is a Kronecker sequence, which is a canonical object in uniform distribution and quasi-Monte Carlo (QMC) theory [19, 45, 46]. From the numerical-integration perspective, it is closely related to lattice rules (rank-1 lattices) and other discrepancy-optimized constructions [47, 48]. For certain function classes (e.g. periodic functions with additional smoothness structure), Fourier-analytic error bounds and specialized QMC designs can yield improved constants or rates compared with a generic bounded-variation/Koksma analysis. The present paper does not benchmark its slice-reconstruction estimator against these classical quadrature baselines.

Transport-based error metrics. Star discrepancy is tailored to interval (or anchored-box) test sets and is therefore coordinate dependent. In contrast, Wasserstein distances provide a geometric notion of equidistribution via optimal transport costs [49, 50]. In one dimension, if μ_N is the empirical measure of the sample points and λ is Lebesgue measure on $[0, 1]$, then

$$W_1(\mu_N, \lambda) = \int_0^1 |F_N(x) - x| \, \mathrm{d}x \le \sup_{x\in[0,1]} |F_N(x) - x| = D_N^*(P_N),$$

so star discrepancy control implies a Wasserstein-1 control. Exploring transport-based bounds (and their robustness properties under coordinate changes) could provide a complementary analysis of the estimator beyond the Koksma framework used here.

D.11 Presentation and notation

The protocol chain benefits from a strict separation between proved statements and interpretive analogies. While the manuscript maintains layer discipline at the logical level, additional editorial standardization would further reduce ambiguity:

- fix notation for arithmetic groups consistently (e.g. $\mathrm{SL}_2(\mathbb{Z})$ and $\mathrm{PSL}_2(\mathbb{Z})$) and standardize matrix conventions;
- standardize constants and admissible ranges for roof/discrepancy parameters whenever they enter quantitative claims;
- make explicit, near each protocol-level bound, which auxiliary constants are available in closed form (as for E_4/E_6) and which remain qualitative.

References

[1] Haobo Ma. Holographic polar arithmetic: Multiplicative ontology, unitary scanning, and the geometric origin of quantum uncertainty. Companion mathematical manuscript, 2025.

[2] Haobo Ma. Omega theory: Axiomatic foundations of holographic spacetime and interactive evolution. Companion physics manuscript, 2025.

[3] Rudolf Haag. *Local Quantum Physics*. Springer, Berlin, 1996.

[4] Ola Bratteli and Derek W. Robinson. *Operator Algebras and Quantum Statistical Mechanics*. Springer, Berlin, 1997.

[5] Raphael Bousso. The holographic principle. *Reviews of Modern Physics*, 74:825–874, 2002.

[6] Ahmed Almheiri, Xi Dong, and Daniel Harlow. Bulk locality and quantum error correction in AdS/CFT. *Journal of High Energy Physics*, 2015(4):163, 2015.

[7] Fernando Pastawski, Beni Yoshida, Daniel Harlow, and John Preskill. Holographic quantum error-correcting codes: Toy models for the bulk/boundary correspondence. *Journal of High Energy Physics*, 2015(6):1–55, 2015.

[8] Daniel Harlow. The ryu–takayanagi formula from quantum error correction. *Communications in Mathematical Physics*, 354(3):865–912, 2017.

[9] Karl Kraus. *States, Effects, and Operations: Fundamental Notions of Quantum Theory*, volume 190 of *Lecture Notes in Physics*. Springer, Berlin, 1983.

[10] Michael A. Nielsen and Isaac L. Chuang. *Quantum Computation and Quantum Information*. Cambridge University Press, Cambridge, 2000.

[11] G. H. Hardy. *Divergent Series*. Clarendon Press, Oxford, 1949.

[12] G. A. Margulis. *Discrete Subgroups of Semisimple Lie Groups*. Springer, Berlin, 1991.

[13] Caroline Series. The modular surface and continued fractions. *Journal of the London Mathematical Society*, 31:69–80, 1985.

[14] Marc A. Rieffel. c^*-algebras associated with irrational rotations. *Pacific Journal of Mathematics*, 93(2):415–429, 1981.

[15] Alain Connes. *Noncommutative Geometry*. Academic Press, 1994.

[16] Arnaud Denjoy. Sur les courbes définies par les équations différentielles à la surface du tore. *Journal de Mathématiques Pures et Appliquées*, 11:333–375, 1932.

[17] Anatole Katok and Boris Hasselblatt. *Introduction to the Modern Theory of Dynamical Systems*. Cambridge University Press, 1995.

[18] Hermann Weyl. Über die gleichverteilung von zahlen mod. eins. *Mathematische Annalen*, 77:313–352, 1916.

[19] L. Kuipers and Harald Niederreiter. *Uniform Distribution of Sequences*. Wiley, New York, 1974.

[20] Marston Morse and Gustav A. Hedlund. Symbolic dynamics II. Sturmian trajectories. *American Journal of Mathematics*, 62(1):1–42, 1940.

[21] M. Lothaire. *Algebraic Combinatorics on Words*. Cambridge University Press, Cambridge, 2002.

[22] Fred Diamond and Jerry Shurman. *A First Course in Modular Forms*. Springer, New York, 2005.

[23] Marius Iosifescu and Cor Kraaikamp. *Metrical Theory of Continued Fractions*. Springer, Dordrecht, 2002.

[24] E. Zeckendorf. Représentation des nombres naturels par une somme de nombres de Fibonacci ou de nombres de Lucas. *Bulletin de la Société Royale des Sciences de Liège*, 41:179–182, 1972.

[25] Tom M. Apostol. *Modular Functions and Dirichlet Series in Number Theory*. Springer, New York, 2 edition, 1990.

[26] Jean-Pierre Serre. *A Course in Arithmetic*. Springer, New York, 1973.

[27] J. F. Koksma. Ein mengentheoretischer satz über die gleichverteilung modulo eins. *Compositio Mathematica*, 2:250–258, 1935.

[28] Haobo Ma. The motive at infinity: Functorialization of the holographic scanning principle, period realizations, and a selection principle. Companion manuscript, 2025.

[29] Maxim Kontsevich and Don Zagier. Periods. In Björn Engquist and Wilfried Schmid, editors, *Mathematics Unlimited – 2001 and Beyond*, pages 771–808. Springer, Berlin, 2001.

[30] Goro Shimura. *Introduction to the Arithmetic Theory of Automorphic Functions*. Princeton University Press, Princeton, 1971.

[31] Pierre Deligne. Valeurs de fonctions l et périodes d'intégrales. In *Automorphic Forms, Representations and L-Functions*, volume 33 of *Proceedings of Symposia in Pure Mathematics*, pages 313–346. American Mathematical Society, Providence, RI, 1979.

[32] Kostas Skenderis. Lecture notes on holographic renormalization. *Classical and Quantum Gravity*, 19(22):5849–5876, 2002.

[33] Pierre Deligne. La conjecture de weil. i. *Publications Mathématiques de l'Institut des Hautes Études Scientifiques*, 43:273–307, 1974.

[34] Daniel Bump. *Automorphic Forms and Representations*. Cambridge University Press, Cambridge, 1997.

[35] Pierre Deligne. Formes modulaires et représentations ℓ-adiques. In *Séminaire Bourbaki, Vol. 1968/69, Exp. 355*, volume 179 of *Lecture Notes in Mathematics*, pages 139–172. Springer, Berlin, 1971.

[36] Michael Harris. Galois representations, automorphic forms, and the sato-tate conjecture. *Indian Journal of Pure and Applied Mathematics*, 45(5):707–746, 2014.

[37] Marc A. Rieffel. Projective modules over higher-dimensional noncommutative tori. *Canadian Journal of Mathematics*, 40(2):257–338, 1988.

[38] John G. Ratcliffe. *Foundations of Hyperbolic Manifolds*. Springer, New York, 1994.

[39] L. Clozel. The sato-tate conjecture. *Current Developments in Mathematics*, 2006(1):1–34, 2006.

[40] Thomas Barnet-Lamb, Toby Gee, and David Geraghty. The sato-tate conjecture for hilbert modular forms. *Journal of the American Mathematical Society*, 24(2), 2011.

[41] Elon Lindenstrauss. Invariant measures and arithmetic quantum unique ergodicity. *Annals of Mathematics*, 163(1):165–219, 2006.

[42] Roman Holowinsky and Kannan Soundararajan. Mass equidistribution for Hecke eigenforms. *Annals of Mathematics*, 172(2):1517–1528, 2010.

[43] P. Arrighi. An overview of quantum cellular automata. *Natural Computing*, 18(4):885–899, 2019.

[44] D. Gross, V. Nesme, H. Vogts, and R. F. Werner. Index theory of one dimensional quantum walks and cellular automata. *Communications in Mathematical Physics*, 310(2):419–454, 2012.

[45] Michael Drmota and Robert F. Tichy. *Sequences, Discrepancies and Applications*, volume 1651 of *Lecture Notes in Mathematics*. Springer, Berlin, 1997.

[46] Harald Niederreiter. *Random Number Generation and Quasi-Monte Carlo Methods*, volume 63 of *CBMS-NSF Regional Conference Series in Applied Mathematics*. SIAM, Philadelphia, 1992.

[47] Ian H. Sloan and Stephen Joe. *Lattice Methods for Multiple Integration*. Cambridge University Press, Cambridge, 1994.

[48] Josef Dick and Friedrich Pillichshammer. *Digital Nets and Sequences: Discrepancy Theory and Quasi-Monte Carlo Integration*. Cambridge University Press, Cambridge, 2010.

[49] Cédric Villani. *Optimal Transport: Old and New*, volume 338 of *Grundlehren der mathematischen Wissenschaften*. Springer, Berlin, 2009.

[50] Filippo Santambrogio. *Optimal Transport for Applied Mathematicians: Calculus of Variations, PDEs, and Modeling*. Birkhäuser, Cham, 2015.